Agricultural and Forest Meteorology 182–183 (2013) 76–90

Contents lists available at ScienceDirect

Agricultural and Forest Meteorology

journal homepage: www.elsevier.com/locate/agrformet

Carbon fluxes, evapotranspiration, and water use efficiency of terrestrial ecosystems in China

Jingfeng Xiao[a,*], Ge Sun[b], Jiquan Chen[c,d], Hui Chen[e], Shiping Chen[f], Gang Dong[g], Shenghua Gao[h], Haiqiang Guo[i], Jixun Guo[j], Shijie Han[k], Tomomichi Kato[l], Yuelin Li[m], Guanghui Lin[n], Weizhi Lu[e], Mingguo Ma[o], Steven McNulty[b], Changliang Shao[f], Xufeng Wang[o], Xiao Xie[i], Xudong Zhang[h], Zhiqiang Zhang[p], Bin Zhao[i], Guangsheng Zhou[f], Jie Zhou[p]

[a] *Earth Systems Research Center, Institute for the Study of Earth, Oceans, and Space, University of New Hampshire, Durham, NH 03824, USA*
[b] *USDA Forest Service, Southern Research Station, Raleigh, NC 27606, USA*
[c] *International Center for Ecology, Meteorology, and Environment, School of Applied Meteorology, Nanjing University of Information Science and Technology, Nanjing, Jiangsu 210044, China*
[d] *Department of Environmental Sciences, University of Toledo, Toledo, OH 43606, USA*
[e] *Key Laboratory of the Ministry of Education for Coastal and Wetland Ecosystems, School of Life Sciences, Xiamen University, Xiamen, Fujian 361005, China*
[f] *State Key Laboratory of Vegetation and Environmental Change, Institute of Botany, Beijing, China*
[g] *School of Life Sciences, Shanxi University, Taiyuan, Shanxi, China*
[h] *Institute of Forestry Research, Chinese Academy of Forestry, Beijing, China*
[i] *Ministry of Education Key Laboratory for Biodiversity Science and Ecological Engineering, Fudan University, Shanghai, China*
[j] *Key Laboratory of Vegetation Ecology, Ministry of Education, Institute of Grassland Sciences, Northeast Normal University, Changchun, China*
[k] *Institute of Applied Ecology, Chinese Academy of Sciences, Shenyang 110016, China*
[l] *Research Institute for Global Change, Japan Agency for Marine-Earth Science and Technology, Yokohama, Japan*
[m] *South China Botanical Garden, Chinese Academy of Sciences, Guangzhou, China*
[n] *Center for Earth System Science, Tsinghua University, Beijing 100084, China*
[o] *Cold and Arid Regions Remote Sensing Observation System Experiment Station, Cold and Arid Regions Environmental and Engineering Research Institute, Chinese Academy of Sciences, Lanzhou 730000, China*
[p] *Ministry of Education Key Laboratory for Soil and Water Conservation and Desertification Combating, Beijing Forestry University, Beijing 100083, China*

ARTICLE INFO

Article history:
Received 27 January 2013
Received in revised form 14 August 2013
Accepted 21 August 2013

Keywords:
Carbon fluxes
Evapotranspiration
Water use efficiency
Eddy covariance
Carbon sink
Synthesis

ABSTRACT

The magnitude, spatial patterns, and controlling factors of the carbon and water fluxes of terrestrial ecosystems in China are not well understood due to the lack of ecosystem-level flux observations. We synthesized flux and micrometeorological observations from 22 eddy covariance flux sites across China, and examined the carbon fluxes, evapotranspiration (ET), and water use efficiency (WUE) of terrestrial ecosystems at the annual scale. Our results show that annual carbon and water fluxes exhibited clear latitudinal patterns across sites. Both annual gross primary productivity (GPP) and ecosystem respiration (ER) declined with increasing latitude, leading to a declining pattern in net ecosystem productivity (NEP) with increasing latitude. Annual ET also generally declined with increasing latitude. The spatial patterns of annual carbon and water fluxes were mainly driven by annual temperature, precipitation, and growing season length. Carbon fluxes, ET, and water use efficiency (WUE) varied with vegetation type. Overall, forest and cropland sites had higher annual fluxes than grassland sites, and the annual fluxes of coastal wetland sites were similar to or slightly higher than those of forest sites. Annual WUE was associated with annual precipitation, GPP, and growing season length. Higher-productivity ecosystems (forests and coastal wetlands) also had higher WUE than lower-productivity ecosystems (grasslands and croplands). The strong relationships between annual GPP and ET demonstrated the coupling of the carbon and water cycles. Our results show that forest plantations had high annual NEP and WUE, and could provide larger carbon sequestration capacity than natural forests. The coastal salt marsh and mangrove ecosystems also had high carbon sequestration capacity. Efforts to strengthen China's terrestrial carbon sink should focus on ecosystems such as forest plantations in southern China where heat and water are ideal for maintaining high productivity. This strategy is especially important because efforts to increase carbon sequestration in areas of limited water may inadvertently contribute to the ongoing water crisis in northern China.
© 2013 Elsevier B.V. All rights reserved.

* Corresponding author. Tel.: +1 603 862 1873.
E-mail address: j.xiao@unh.edu (J. Xiao).

0168-1923/$ – see front matter © 2013 Elsevier B.V. All rights reserved.
http://dx.doi.org/10.1016/j.agrformet.2013.08.007

1. Introduction

China's terrestrial ecosystems play an important role in regulating the terrestrial carbon and water cycles. China is now one of the world's top emitters of greenhouse gases that directly contribute to global warming (IPCC, 2007). The carbon sequestration potential of terrestrial ecosystems is increasingly recognized as one of the strategies for slowing down the buildup of carbon dioxide (CO_2) in the atmosphere and mitigating climate change in China (Lu et al., 2012). There is general agreement that as a whole, terrestrial ecosystems in China provide a significant carbon sink (Fang et al., 2001; Piao et al., 2009; Xiao et al., 2009; Pan et al., 2011; Tian et al., 2011) and regulate the hydrological cycle (Wei et al., 2005; Sun et al., 2006; Gao et al., 2007). However, the magnitude, spatial patterns, and controlling factors of the carbon and water fluxes of terrestrial ecosystems across China are not well understood due to the lack of ecosystem-level flux observations.

The eddy covariance (EC) technique provides a valuable approach for measuring carbon and water fluxes at the ecosystem level. The EC flux towers have provided continuous measurements of net ecosystem exchange (NEE) and evapotranspiration (ET, or latent heat flux) since the early 1990s (Wofsy et al., 1993; Baldocchi et al., 2001). NEE is equal to net ecosystem productivity (NEP) but has the opposite sign (NEP = −NEE). The NEE measurements are routinely partitioned into its two components: gross primary productivity (GPP) and ecosystem respiration (ER). ET represents latent heat flux, and is a key component of water and energy balance. EC flux observations have been widely used to examine ecosystem carbon fluxes (Baldocchi, 2008; Amiro et al., 2010; Schwalm et al., 2010), ET (Ryu et al., 2008; Khatun et al., 2011), and water use efficiency (WUE) (Ponton et al., 2006; Yu et al., 2008a) worldwide. Flux observations have also been upscaled to assess terrestrial carbon and water dynamics at regional, continental, and global scales (Xiao et al., 2008, 2010, 2011, 2012; Sun et al., 2011a). Previous studies have shown the close coupling of carbon and water cycles and the advantages of measuring both fluxes simultaneously in understanding the interactions of carbon and water at ecosystem to regional scale (Law et al., 2002; Niu et al., 2008; Beer et al., 2009).

There are currently over 200 EC flux sites in China. Flux observations have been used to examine carbon and water fluxes at individual sites and across multiple sites in China using observations from a very limited number (typically 1–6) of sites (Kato et al., 2004; Hu et al., 2008; Yu et al., 2008a,b; Dong et al., 2011). China has an enormous land area (~9.6 million km^2) and encompasses a large range of ecosystem and climate types. The use of observations from a number of sites across China is essential for assessing the carbon and water budgets of terrestrial ecosystems in China, particularly the variation within and across ecosystem types. A recent synthesis study of the spatial patterns and climatic controls of carbon fluxes (Yu et al., 2013) represents the most comprehensive evaluation to date in China. However, to our knowledge, no study has yet examined carbon fluxes, ET, and the coupling of carbon and water cycles (e.g., WUE) in China using observations from a number of sites encompassing a range of ecosystem and climate types.

Despite the large number of flux sites, the availability and sharing of flux data remain a major challenge for synthesis studies in China (Paw U, 2006). Unlike the United States, Europe, and Canada, China has not established a nationwide flux network that coordinates the collection, analysis, and distribution of observations from sites across the country. Most flux sites are instrumented and operated by different organizations (e.g., Chinese Academy of Forestry Sciences, the Chinese Academy of Meteorological Sciences), universities (e.g., Beijing Forestry University, Xiamen University, Fudan University), and institutes of Chinese Academy of Sciences (e.g., the Institute of Botany, Cold and Arid Regions Environmental and Engineering Research Institute, Institute of Geographical Sciences and Natural Resources, and Institute of Shenyang Applied Ecology). Unlike AmeriFlux, the official ChinaFlux (Yu et al., 2006) coordinates a relatively limited number (8–12) of sites. The lack of data sharing has hindered the progress of ecosystem-level carbon and water cycle and synthesis studies in China (Paw U, 2006).

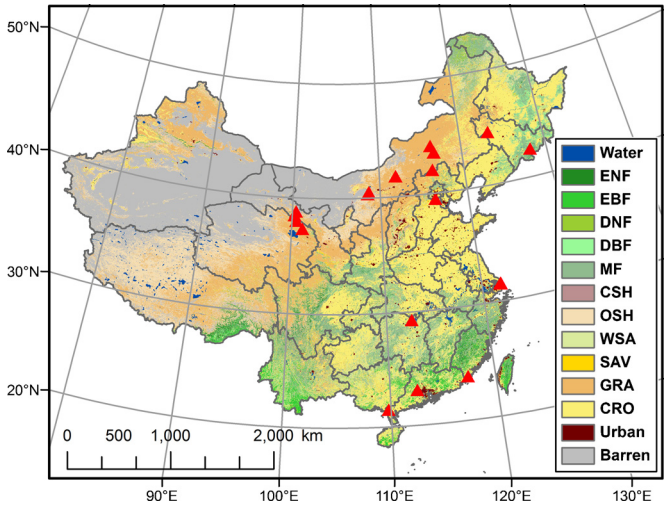

Fig. 1. Location and distribution of the eddy covariance (EC) flux sites used in this study. The base map is the 1 km land-cover map derived from the moderate resolution imaging spectroradiometer (MODIS) (Friedl et al., 2002). The land-cover types of the map are evergreen needleleaf forests (ENF), evergreen broadleaf forests (EBF), deciduous needleleaf forests (DNF), deciduous broadleaf forests (DBF), mixed forests (MF), closed shrublands (CSH), open shrublands (OSH), woody savannas (WSA), savannas (SAV), grasslands (GRA), croplands (CRO), urban, barren or sparsely vegetated (Barren), and water. The symbols represent the EC sites, and the site descriptions are provided in Tables 1 and 2.

In this study, we synthesized flux observations from 22 EC flux sites encompassing a range of climate and ecosystem types across China, and examined annual carbon fluxes, ET, and WUE of terrestrial ecosystems. This synthesis is the outcome of the initiative of the U.S.-China Carbon Consortium (USCCC) to facilitate the sharing of flux observations for synthesis studies. The USCCC is a grassroots organization that coordinates ecologists who instrument and maintain EC flux towers for ecosystem studies and scientists who are interested in synthesis studies in the U.S. and China (Sun et al., 2009). This synthesis is the first effort to examine carbon fluxes, ET, and WUE of terrestrial ecosystems in China using data from so many flux sites encompassing a range of climate and ecosystem types.

The overall goal of our study is to examine the magnitude, spatial patterns, and climate regulation of carbon fluxes, ET, and WUE of terrestrial ecosystems in China. The specific objectives of our study are to (1) synthesize flux measurements from 22 sites across China by building a database with flux and meteorology data, (2) examine the magnitude and spatial patterns of carbon fluxes, ET, and WUE and identify their key climatic controls at the national scale, and (3) better understand the interactions between GPP, ET, and WUE across ecosystems.

2. Materials and methods

We compiled flux and micrometeorological observations from a total of 22 EC flux sites across China (Tables 1 and 2; Fig. 1). These sites encompass four major vegetation types: forests, grasslands, croplands, and coastal wetlands. All 22 sites, except Dinghushan (DHS), Changbaishan (CBS), and Haibei Alpine Tibet site (HB), are affiliated with the USCCC. The 22 sites consist of 6 forest sites, 9 grassland sites, 2 cropland sites, and 5 coastal wetland sites. The site descriptions for all 22 sites including name, location, vegetation

Table 1
Site descriptions including name, latitude, longitude, vegetation type, years of data available, and references for each flux site. These sites involve seven IGBP (International Geosphere-Biosphere Program) vegetation types: evergreen broadleaf forests (EBF), evergreen needleleaf forests (ENF), deciduous broadleaf forests (DBF), mixed forests (MF), grasslands (GRA), croplands (CRO), and wetlands (WET).

Broad vegetation type	Site name	Province	Lat (°N)	Lon (°E)	Vegetation_type	IGBP	Temperature (°C)	Precipitation (mm)	Duration	Reference
Forests	Daxing (DX)	Beijing	39.53	116.25	Populus euramericana	DBF	11.5	569	2006–2009	Liu et al. (2009)
	Dinghushan (DHS)	Guangdong	23.17	112.53	Evergreen broadleaf forest	EBF	22.3	1678	2003–2005	Zhou et al. (2011)
	Changbaishan (CBS)	Jilin	42.40	128.10	Temperate mixed forest	MF	3.6	695	2003	Guan et al. (2006)
	Guantan (GT)	Gansu	38.53	100.25	Qignhai spruce (Picea crassifolia)	ENF	3.2	334	2010	
	Hunan Yueyang (YY)	Hunan	29.31	112.51	Poplar plantation	DBF	16.8	1309	2005–2006	Wei et al. (2012)
	Kubuqi populus forest (KBQ)	Inner Mongolia	40.54	108.69	Poplar plantation	DBF	6.3	318	2005–2006	Wilske et al. (2009)
Grasslands	Arou (AR)	Qinghai	38.04	100.46	Alpine meadow	GRA	0.9	403	2008–2009	Wang et al. (2012)
	Changling (CL)	Jilin	44.58	123.50	Temperate meadow steppe	GRA	5.0	400	2007–2010	Dong et al. (2011)
	Duolun grassland (DL1)	Inner Mongolia	42.05	116.28	Typical steppe	GRA	1.6	385	2006–2007	Chen et al. (2009)
	Haibei Alpine Tibet site (HB)	Qinghai	37.37	101.18	Alpine meadow	GRA	-1.7	561	2002–2004	Kato et al. (2006)
	Siziwang fenced (SZW1)	Inner Mongolia	41.79	111.89	Desert steppe	GRA	3.4	325	2010	Shao et al. in press
	Siziwang grazed (SWZ2)	Inner Mongolia	41.79	111.90	Degraded desert steppe	GRA	3.4	325	2010	Shao et al. in press
	Xilinhot grassland site (XLH1)	Inner Mongolia	43.55	116.67	degraded typical steppe	GRA	2.0	350	2006–2007	Chen et al. (2009)
	Xilinhot fenced steppe (XLH2)	Inner Mongolia	43.55	116.68	Typical steppe	GRA	2.0	350	2006–2007	Chen et al. (2009)
	Xilinhot fenced typical steppe (XFS)	Inner Mongolia	44.13	116.33	Short grass steppe	GRA	2.0	290	2004–2006	Wang et al. (2008)
Croplands	Duolun cropland (DL2)	Inner Mongolia	42.05	116.28	Cropland	CRO	1.6	385	2006–2007	Chen et al. (2009)
	Yingke (YK)	Gansu	38.86	100.41	Wheat, maize	CRO	7.2	127	2009–2010	Wang et al. (2012)
Coastal wetlands	Dongtan1 (DT1)	Shanghai	31.52	121.96	Coastal salt marsh	WET	16.2	1095	2005–2007	Guo et al. (2009)
	Dongtan2 (DT2)	Shanghai	31.58	121.90	Coastal salt marsh	WET	16.2	1095	2005–2007	Yan et al. (2008)
	Dongtan3 (DT3)	Shanghai	31.52	121.97	Coastal salt marsh	WET	16.2	1095	2005–2007	Guo et al. (2009)
	Gaoqiao (GQ)	Guangdong	21.57	109.76	Mangroves	WET	22.9	1770	2010	
	Yunxiao (YX)	Fujian	23.92	117.42	Mangroves	WET	21.1	1286	2010	

type, years of data available, and references are provided in Table 1, and the site information on dominant species, climate type, soil type, canopy height, aboveground biomass, leaf area index (LAI), and stand age are summarized in Table 2.

2.1. Forest sites

Two forests sites are located in the subtropical zone – DHS and Yueyang (YY). The DHS site (Zhou et al., 2011; Li et al., 2012) is located in the Dinghushan Biosphere Reserve in Guangdong Province. The YY site (Wei et al., 2012) is located on a floodplain of the Yangtze River in the northern part of Hunan Province. Two forest sites are located in the temperate zone – Daxing (DX) and CBS. The DX site (Liu et al., 2009) is located in a managed pure poplar plantation in Daxing Forestry Farm of Beijing. The CBS site (Guan et al., 2006) is located within the National Natural Conservation Park of the Changbai Mountain in northeastern China. One forest site – Kubuqi (KBQ) (Wilske et al., 2009) is within the semiarid zone and is located in the Kubuqi Desert. The Guantan site (GT) is within the subalpine zone, and is located in the Dayekou watershed in middle reaches of the Heihe River.

Among these sites, YY, DX, and KBQ are forest plantations, and other sites (DHS, CBS, and GT) are natural forests. DX is a *Populus euramericana* plantation and was established in 1998. YY is located in a *Populus deltoides* plantation, which was established in 2000. KBQ is a seven-year-old poplar plantation (*Populus* sp.).

2.2. Grasslands sites

Six of the grassland sites are located in Inner Mongolia. The Duolun grassland site (DL1) (Chen et al., 2009) is located within a typical semi-arid, agro-pastoral transit zone between

Table 2
Site descriptions including dominant species, climate type, soil type, mean canopy height, aboveground biomass, maximum leaf area index (LAI), and stand age. Abbreviations are used for site names here, and full site names are provided in Table 1. Stand age information is as of 2013.

Broad vegetation type	Site name	Dominant species	Climate type	Soil type	Canopy height (m)	Aboveground biomass ($g C m^{-2}$)	LAI	Stand age (yrs)
Forests	DX	*Populus euramericana* cv. "74/76"	Temperate continental climate	Sandy soil	14.8	1300	3.1	11
	GT	Picea crassifolia		Silt loam	18–20	6000	5.8	~90
	DHS	*Schima superba*, *Castanopsis chinensis*, *Pinus massonian*	Subtropical monsoon humid climate	Lateritic red earth	17	15,000	6.5	~100
	CBS	*Pinus koriaensis*, *Tilia amurensis*, *Acer mimo*, *Fraxinus mandshurica*, *Quercus mongolica*, *Ulmus glabra*	Monsoon-influenced, temperate continental climate	Montane dark Brown forest soil	23–28	16,800	5.8	~450
	YY	*Populus deltoides*	Subtropical monsoon climate	Fluvo-aquic soil	19.5	1807.5		7[a]
Grasslands	KBQ	Populus sp.	Semiarid, continental climate	Sandy soil	2.2		0.4	10
	AR		Alpine climate	Clay loam	0.15–0.30	105	2.5	
	CL	*Leymus chinensis*, *Phragmitis communis*.	Temperate, semi-arid continental monsoon climate	Alkali-saline soil	0.7–0.8	336.3	3.1	
	DL1	*Stipa krylovii*, *Agropyron cristatum*, *Artemisia frigida*, *Cleistogenes squarrosa*, *Leymus chinensis*	Semi-arid, continental monsoon climate	Chestnut soil	0.4	106.9	1.0	
	HB	*Kobresia humilis*, *K. pygmaea*, and *K. tibetica* (Cyperaceae)	Alpine climate	Clay loam		342	3.8	
	SZW1	*Stipa breviflora*	Temperate continental monsoon climate	Chenozemic soil	0.25	118	0.7	
	SWZ2	*Stipa breviflora*	Temperate continental monsoon climate	Chenozemic soil	0.08	81	0.6	
	XLH1	*Stipa grandis* and *Leymus chinensis*	Semi-arid, continental monsoon climate	Chestnut soil	0.3	84.8	0.7	
	XLH2	*Stipa grandis* and *Artemisia frigid*	Semi-arid, continental monsoon climate	Chestnut soil	0.5	99.8	0.5	
	XFS	*Stipa krylovii*, *Leymus chinensis*	Semi-arid, continental monsoon climate	Chestnut soil	0.35	180	1.0	
Croplands	DL2	*Triticum aestivum* L.), *Avena nuda* L., *Fagopyrum esculentum Moench*	Semi-arid, continental monsoon climate	Chestnut soil	0.6	330.2	2.4	
	YK	*Triticum aestivum*, *Zea mays*	Continental, arid climate	Silt loam	1.0–1.8	1950	5.4	
Coastal wetlands	DT1	*Spartina alterniflora*, *Phragmites australis*	Subtropical monsoon climate	Solonchaks	1.5–2.5	1170.0	4.7	
	DT2	*Spartina alterniflora*, *Phragmites australis*	Subtropical monsoon climate	Solonchaks	1.5–2.5	765.6	3.8	
	DT3	*Spartina alterniflora*, *Phragmites australis*, *Scirpus mariqueter*	Subtropical monsoon climate	Solonchaks	1.5–2.5	400.7	1.6	
	GQ	*Aegiceras corniculatum*, *Bruguiera gymnorrhiza*	Tropical and subtropical monsoon climate	Silty clay soil	3.0	38,600	4.4	100
	YX	*Kandelia obovata*, *Avicennia marina*	Tropical and subtropical monsoon climate	Silty clay soil	4.4	16,400	2.6	30–40

[a] The stand age of YY is as of 2006. The stand is now replaced with populous seedlings.

the North China Plain and Inner Mongolia. The EC tower is instrumented within a permanent study plot (>50 ha) that is fenced in 2001 to exclude from grazing. The Xilinhot grassland site (XLH1) and the Xilinhot fenced site (XLH2) (Chen et al., 2009) are located in the typical steppe zone. XLH1 has been grazed, while XLH2 has been fenced to exclude from grazing since 1999. The Xilinhot fenced typical steppe site (XFS) (Wang et al., 2008) is approximately 24 km to the northeast of Xilinhot City. The Siziwang fenced (SZW1) and grazed (SZW2) sites (Shao et al., 2013) are located in Siziwang Banner. SZW1 has been fenced (500 m × 100 m), and SZW2 has been grazed (stocking rate: 5–10 sheep-unit-month ha^{-1}) year round under collective sheep grazing for over 30 years.

The Changling (CL) site (Dong et al., 2011) is located in Jilin Province. CL is on a northern meadow on the southern Songnen Plain. This site is managed by the Songnen Grassland Ecology Field Station of the Northeast Normal University. The A'rou (AR) site (Wang et al., 2012) is located in the A'rou freeze/thaw observation station in an area of alpine meadow in the upper stream of the Heihe River. Seasonally frozen soil is widely distributed in this

region. The Haibei Alpine Tibet (HB) site (Kato et al., 2006) is instrumented at the Haibei Alpine Meadow Ecosystem Research Station. The station is located in a valley surrounded by the Qilian Mountains on the northeast Tibet and has an average elevation of 4000 m. This site is grazed by yaks and sheep every winter.

2.3. Cropland sites

We used flux observations from two cropland sites – the Yingke oasis site (YK) and the Duolun cropland site (DL2). The YK site (Wang et al., 2012) is located in an oasis in the middle reaches of the Heihe River, and is surrounded by the Gobi desert. YK is in an irrigated field, and the crops are spring wheat (May–July) and maize (August–September). The DL2 site (Chen et al., 2009) is located within a semi-arid, agro-pastoral transit zone between the North China Plain and Inner Mongolia. This cropland site has been cultivated for 38 years. Before cultivation, this site was a steppe used for grazing. Unlike YK, DL2 is not irrigated.

2.4. Coastal wetland sites

The five wetland sites consist of 3 coastal salt marsh sites and 2 mangrove sites. The three coastal salt marsh sites – Dongtan 1 (DT1), Dongtan 2 (DT2), and Dongtan 3 (DT3) (Yan et al., 2008; Guo et al., 2009) are located on the east shore of Dongtan, the largest wetland (ca. 230 km^2) in the Yangtze River estuary, on the Chongming Island in Shanghai. Tidal movement at Dongtan is regular and semidiurnal. The two mangrove sites – Yunxiao (YX) and Gaoqiao (GQ) are located on the southern coast in Fujian and Guangdong provinces, respectively. YX is located in the Zhangjiangkou Mangrove Nature Reserve, and GQ is instrumented in the Zhanjiang Mangrove Nature Reserve.

2.5. Flux observations and synthesis

We compiled daily, gap-filled fluxes and micrometeorological data from all the 22 sites. The micrometeorological variables consist of air temperature, precipitation, vapor pressure deficit (VPD), and photosynthetically active radiation (PAR). For each site, the daily, gap-filled fluxes and micrometeorological data were aggregated to the annual scale to calculate annual sums of carbon fluxes (GPP, ER, and NEP; $g\,C\,m^{-2}\,yr^{-1}$), precipitation ($mm\,yr^{-1}$), and ET ($mm\,yr^{-1}$) and annual averages of temperature (°C), PAR ($MJ\,m^{-2}\,day^{-1}$), and VPD (kPa). For NEP, positive values indicate net carbon uptake, and negative values indicate net carbon release. NEP is equal to NEE but has opposite sign to NEE. For each site, the daily, gap-filled GPP data was used to determine the green-up (or leaf-out) date, the senescence date, and the growing season length (GSL). The green-up date was determined as the first day that GPP exceeded $1.0\,g\,C\,m^{-2}\,day^{-1}$ and GPP also exceeded this rate during the following two weeks. The senescence date was determined as the first day that GPP became lower than $1.0\,g\,C\,m^{-2}\,day^{-1}$ and GPP declined from this rate during the following two weeks. GSL was calculated as GSL = senescence date – green-up date + 1.

We analyzed the magnitude and spatial patterns of annual carbon fluxes, ET, and WUE, and examined the variability of carbon and water fluxes within and across vegetation types: forests, coastal wetlands, croplands, and grasslands. Annual WUE is defined as the ratio of annual GPP and annual ET (i.e., GPP/ET, $g\,C\,kg^{-1}\,H_2O$). We also analyzed the spatial patterns of phenological stages (green-up date and senescence date) and their variability across sites and vegetation types. We then examined the regulatory mechanisms of carbon and water fluxes by micrometeorological variables (temperature, precipitation, VPD, and PAR) and GSL.

3. Results

3.1. Carbon fluxes

Fig. 2 illustrates the annual GPP, ER, and NEP for each site. The mean annual carbon fluxes of each year are also summarized in Table 3. The magnitude of annual carbon fluxes varied with site and vegetation type (Fig. 2). The annual GPP of forest sites ranged from 424 to 2166 $g\,C\,m^{-2}\,yr^{-1}$. Among these sites, YY had the highest annual GPP; DX and DHS had intermediate GPP; CBS had the lowest annual GPP. Similarly, annual ER varied substantially among sites, ranging from 369 to 1291 $g\,C\,m^{-2}\,yr^{-1}$. The annual NEP of forest sites varied from 55 to 874 $g\,C\,m^{-2}\,yr^{-1}$. YY had the highest annual NEP; DHS had intermediate NEP; CBS had the lowest NEP. The annual NEP of DX was lower than 400 $g\,C\,m^{-2}\,yr^{-1}$ in 2006 and 2007 but reached 791 $g\,C\,m^{-2}\,yr^{-1}$ in 2008.

The annual GPP of the coastal wetland sites was typically between 1500 and 2000 $g\,C\,m^{-2}\,yr^{-1}$, and was slightly higher than that of the forested sites except YY (Fig. 2). The mangrove sites (YX and GQ) had similar annual GPP to the coastal marsh sites (DT1, DT2, and DT3). The annual NEP of these coastal wetlands sites were between 600 and 800 $g\,C\,m^{-2}\,yr^{-1}$ with the exception of 2005 for DT2 (403 $g\,C\,m^{-2}\,yr^{-1}$). The annual NEP of the coastal wetland sites was comparable to that of the forest plantation sites.

For the croplands, YK had a GPP of ~1500 $g\,C\,m^{-2}\,yr^{-1}$ that was comparable to that of two forest sites – DX and DHS (Fig. 2). However, the annual GPP of DL2 was lower than 500 $g\,C\,m^{-2}\,yr^{-1}$. The annual NEP of YK was 631 and 701 $g\,C\,m^{-2}\,yr^{-1}$ in 2008 and 2009, respectively, and these values were similar to those of the forest and coastal wetland sites. YK also had much higher annual NEP than DL2 (97 and 55 $g\,C\,m^{-2}\,yr^{-1}$ in 2006 and 2007, respectively).

Among the grassland sites, AR had the highest annual GPP (803 $g\,C\,m^{-2}\,yr^{-1}$), followed by HB and CL; and XFS had the lowest GPP (81–184 $g\,C\,m^{-2}\,yr^{-1}$) (Fig. 2). On average, CL and AR had higher annual NEP than other grassland sites. The annual NEP of the grassland sites was typically lower than 130 $g\,C\,m^{-2}\,yr^{-1}$, which was much lower than that of the forest, coastal wetland, and cropland sites.

Among the 22 sites, GT, KBQ, SZW1, SZW2, XLH1, and XLH2 had flux observations for the growing season only (Table 3). For the two forest sites, GT had high GPP and NEP, while Kubuqi desert site – KBQ had very low GPP and NEP. XLH2 had much higher GPP and ER than the Siziwang sites – SZW1 and SWZ2, while XLH2 slightly released carbon into the atmosphere over the growing season (28.3 $g\,C\,m^{-2}$).

Some sites exhibited significant interannual variability in annual GPP (Fig. 2). For example, DX had the lowest annual GPP (1319 $g\,C\,m^{-2}\,yr^{-1}$) in 2007 and the highest annual GPP (1653 $g\,C\,m^{-2}\,yr^{-1}$) in 2008 with a relative change of 25.3% from 2007 to 2008. Overall, the grassland sites showed significant year-to-year variability. For instance, the annual GPP of DL1 in 2006 was approximately twice as much as that of 2007. Some sites had little interannual variability. For example, DHS exhibited little interannual variation in GPP.

Similarly, some flux sites exhibited large interannual variability in annual NEP (Fig. 2). For instance, DX had the lowest annual NEP in 2007 (373 $g\,C\,m^{-2}\,yr^{-1}$) and had the highest NEP in 2008 (791 $g\,C\,m^{-2}\,yr^{-1}$), with a twofold change from 2007 to 2008. For DT1, the difference in annual NEP between 2005 (or 2007) and 2006 was nearly 200 $g\,C\,m^{-2}\,yr^{-1}$. For DT2, the annual net carbon uptake in 2006 was approximately twice as much as during 2005. The annual NEP of HB was 30 and 137 $g\,C\,m^{-2}\,yr^{-1}$ in 2002 and 2003, respectively, and the much lower net carbon uptake in 2002 was due to much lower GPP and higher ER in 2002 relative to 2003. As with GPP, NEP exhibited little year-to-year variation for DHS and YK.

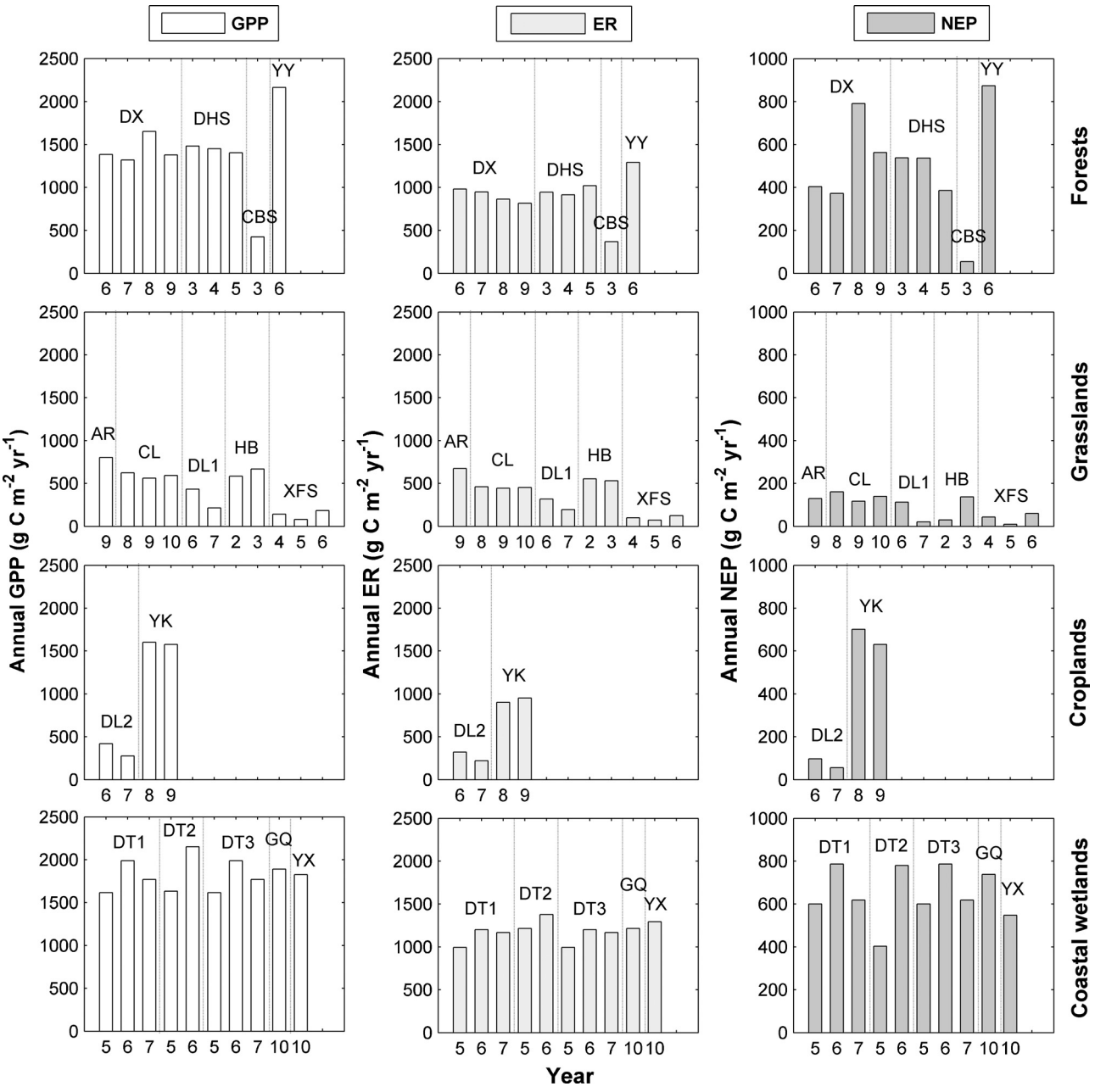

Fig. 2. Annual GPP, ER, and NEP for each eddy covariance site within each vegetation type: (a) forests; (b) grasslands; (c) croplands; (d) coastal wetlands.

Annual carbon fluxes exhibited latitudinal patterns across sites (Fig. 3). Both annual GPP and ER decreased with increasing latitude across these sites. Overall, lower-latitude sites had higher fluxes, while higher-latitude sites had lower fluxes. As a result, the net carbon uptake – annual NEP also declined with increasing latitude. Annual carbon fluxes exhibited no longitudinal dependency.

3.2. Climate regulation of carbon fluxes

Mean annual temperature and precipitation varied across sites (Fig. 3), ranging from −0.8 to 23.4 °C and from 68 to 1944 mm, respectively. Mean PAR ranged from 4.1 to 8.1 MJ m^{-2} day^{-1}. Mean annual temperature and precipitation exhibited strong latitudinal patterns (Fig. 3). Both temperature and precipitation generally declined with increasing latitude. Overall, lower-latitudes sites were warmer and wetter, while higher-latitude sites were colder and drier. By contrast, PAR and VPD did not significantly vary with latitude across these sites.

Similarly, these flux sites varied in the green-up date, senescence date, and GSL (Table 3; Fig. 3). Both green-up and senescence dates exhibited clear latitudinal patterns (Fig. 3). The green-up date was positively correlated with latitude, showing that lower-latitude ecosystems had earlier leaf-out, and higher-latitude sites had later leaf-out. The senescence date was negatively correlated with latitude, indicating that the tropical and subtropical sites had later senescence date, while cold temperate and subalpine ecosystems had earlier senescence date. The latitudinal patterns of green-up and senescence dates resulted in a declining trend in GSL with increasing latitude (Fig. 3). The tropical and subtropical sites had the longest growing season; the temperate sites had intermediate GSL; and the cold temperate and subalpine sites had the shortest growing season. The forest ecosystem at DHS and the mangrove sites (GQ and YX) photosynthesize throughout the year.

Table 3
Mean annual carbon fluxes, ET, WUE, green-up date, senescence date, and GSL for each site. The numbers with * are values for the growing season. Abbreviations are used for site names here, and full site names are provided in Table1.

Broad vegetation type	Site name	GPP ($g C m^{-2} yr^{-1}$)	ER ($g C m^{-2} yr^{-1}$)	NEP ($g C m^{-2} yr^{-1}$)	ET (mm)	WUE ($g C kg^{-1} H_2O$)	Green-up date	Senescence date	GSL (days)
Forests	DX	1434.4	901.9	532.6	585.6	2.45	100	304	205
	GT	1107.1*	550.2*	556.8*	308.0*	3.59*	75	301	227
	DHS	1446.5	959.5	487.0	630.0	2.30	1	365	365
	CBS	423.6	368.8	54.82	150.5	2.81	145	273	129
	YY	2166.2	1292.1	874.0	957.8	2.26	59	327	269
	KBQ	164.1*	87.7*	76.3*	187.8*	0.87*	153	257	105
Grasslands	AR	802.6	673.0	129.7			134	284	151
	CL	592.0	452.9	139.1	390.6	1.52	139	266	128
	DL1	323.3	256.5	66.9	367.3	0.88	150	254	105
	HB	626.2	542.5	83.7	363.2	1.72	143	277	135
	SZW1	62.4*	54.5*	7.9*	71.8*	0.87*	217	261	45
	SWZ2	124.9*	96.4*	28.5*	116.5*	1.07*	213	273	61
	XLH1			104.6*	132.7*		147	230	84
	XLH2	483.7*	512.7*	−28.3*	175.7*	2.76*	159	265	107
	XFS	135.6	98.1	37.5	287.1	0.47	183	228	46
Croplands	DL2	346.9	270.7	76.2	327.6	1.06	159	238	80
	YK	1589.2	926.4	666.1			115	285	171
Coastal wetlands	DT1	1791.2	1121.0	668.7	616.8	2.90	94	340	247
	DT2	1891.0	1296.1	591.3	646.9	2.92	95	337	243
	DT3	1791.2	1121.0	668.7	609.8	2.94	94	340	247
	GQ	1952.6	1215.0	737.7	939.4	2.01	1	365	365
	YX	1842.6	1294.7	547.9	865.8	2.11	1	365	365

Annual carbon fluxes exhibited strong relationships with annual temperature, precipitation and GSL (Fig. 4). Specifically, both GPP and ER were positively related to annual temperature and precipitation across these sites. Compared to precipitation, temperature had a stronger correlation with GPP and ER. Both GPP and ER were also strongly correlated with GSL. Annual NEP was also positively related to annual temperature and precipitation, showing that higher air temperature and/or precipitation led to higher net carbon uptake. There was also a significant relationship between annual NEP and GSL. Annual carbon fluxes were not significantly correlated with PAR or VPD across sites.

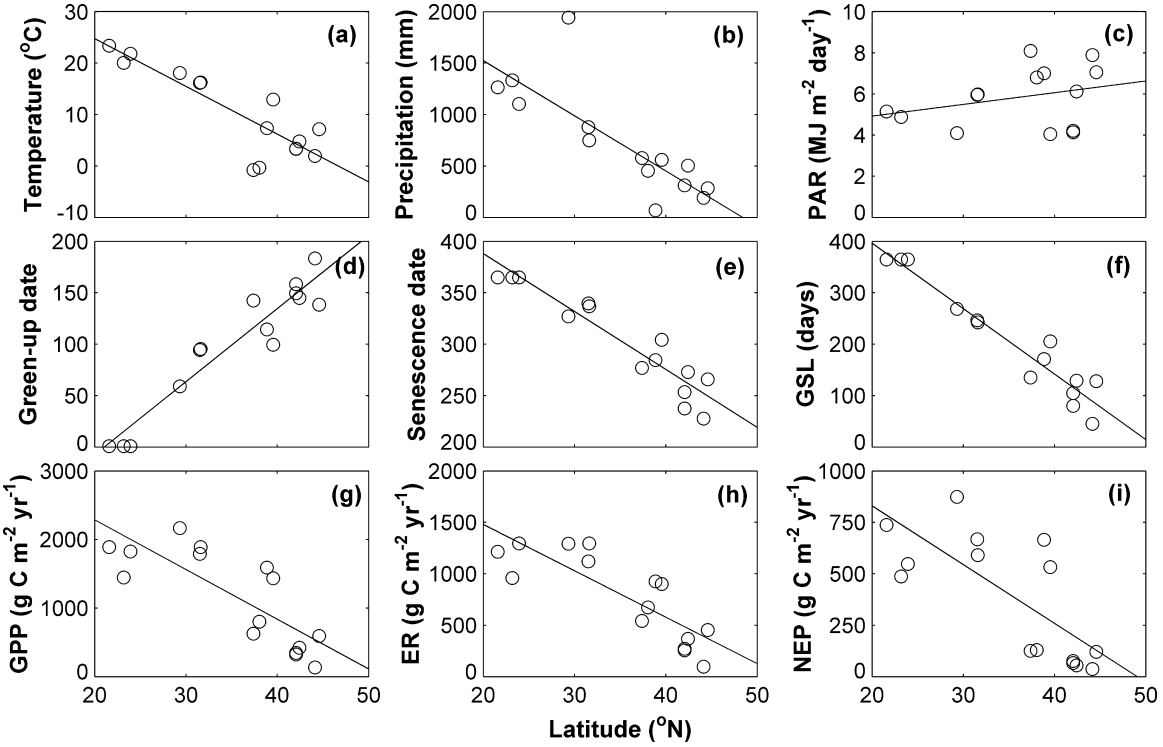

Fig. 3. Latitudinal patterns of climate variables, phenological stages, growing season length (GSL), and carbon fluxes: top panels – (a) annual temperature ($y = -0.93x + 43.37$, $R^2 = 0.76$, $p < 0.001$), (b) annual precipitation ($y = -53.61x + 2595.1$, $R^2 = 0.68$, $p < 0.001$), and (c) annual PAR ($y = 0.057x + 3.79$, $R^2 = 0.09$, $p = 0.27$) against latitude; middle panels – (d) green-up date ($y = 7.10x - 149.46$, $R^2 = 0.90$, $p < 0.001$), (e) senescence date ($y = -5.63x + 500.64$, $R^2 = 0.88$, $p < 0.001$), and (f) GSL ($y = -12.73x + 651.10$, $R^2 = 0.93$, $p < 0.001$) against latitude; and bottom panels – (g) annual GPP ($y = -72.49x + 3736.8$, $R^2 = 0.64$, $p < 0.001$), (h) annual ER ($y = -45.13x + 2383.5$, $R^2 = 0.69$, $p < 0.001$), and (i) annual NEP ($y = -28.56x + 1401.7$, $R^2 = 0.55$, $p < 0.01$) against latitude.

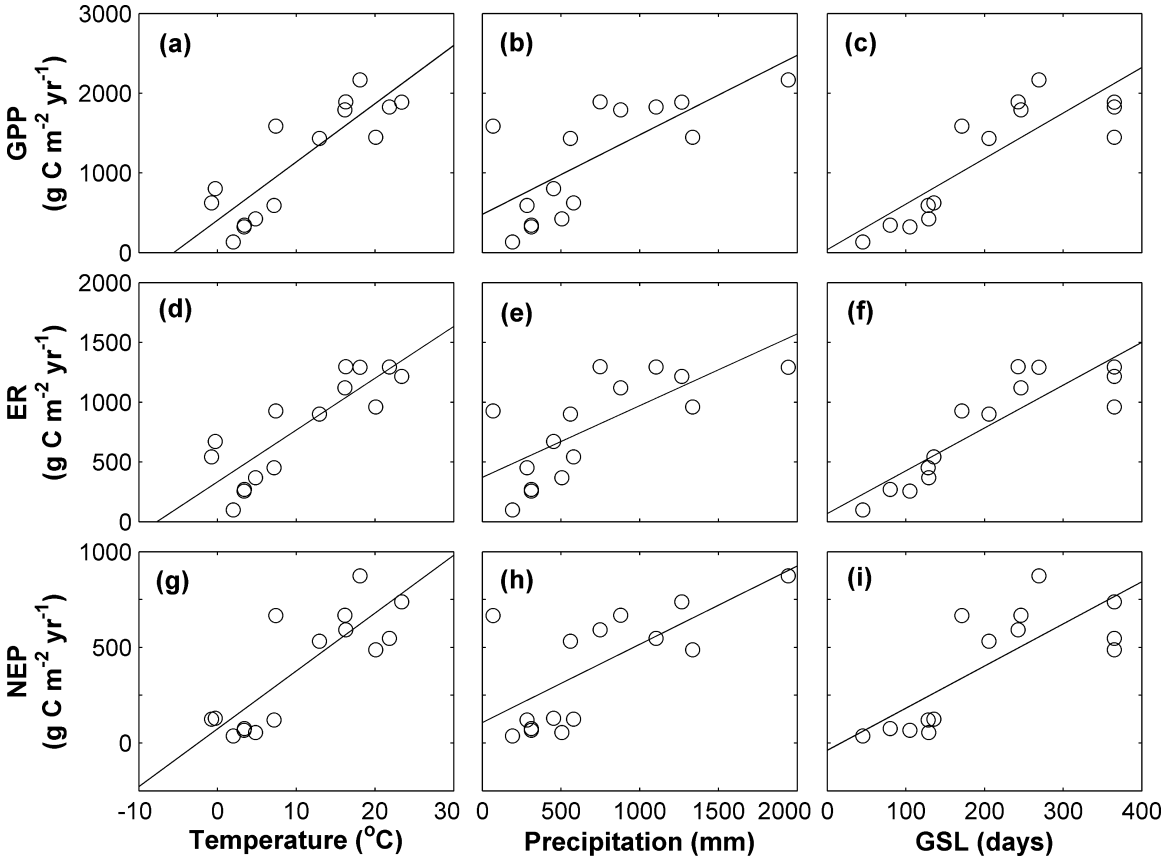

Fig. 4. Relationships between annual carbon fluxes and climate variables across sites: top panels – annual GPP versus (a) annual temperature ($y = 73.06x + 406.93$, $R^2 = 0.74$, $p < 0.001$), (b) annual precipitation ($y = 1.00x + 480.00$, $R^2 = 0.51$, $p < 0.01$), and (c) GSL ($y = 5.72x + 37.20$, $R^2 = 0.70$, $p < 0.001$); middle panels – annual ER versus (d) annual temperature ($y = 43.31x + 333.83$, $R^2 = 0.73$, $p < 0.001$), (e) annual precipitation ($y = 0.60x + 371.17$, $R^2 = 0.52$, $p < 0.01$), and (f) GSL ($y = 3.58x + 67.79$, $R^2 = 0.76$, $p < 0.001$); bottom panels – annual NEP versus (g) annual temperature ($y = 30.25x + 73.93$, $R^2 = 0.70$, $p < 0.001$), (h) annual precipitation ($y = 0.41x + 107.31$, $R^2 = 0.47$, $p < 0.01$), and (i) GSL ($y = 2.20x - 38.16$, $R^2 = 0.60$, $p < 0.001$).

3.3. Evapotranspiration (ET)

Similar to carbon fluxes, annual ET also varied with vegetation type (Table 3; Fig. 5). Among all the sites, YY had the highest annual ET (958 mm yr^{-1}) and CBS had the lowest ET (151 mm yr^{-1}) (Fig. 5). Overall, the higher-productivity forest (DX, DHS, and YY) and coastal wetland (YX, GQ, DT1, DT2, and DT3) sites had higher annual ET (~600–1000 mm yr^{-1}) than lower-productivity grassland and cropland sites (~200–400 mm yr^{-1}). Six of the 22 sites (GT, KBQ, SZW1, SZW2, XLH1, and XLH2) measured ET for the growing season only, and the growing season ET ranged from 70 to 310 mm (Table 3).

For a given vegetation type, annual ET also varied with site (Fig. 5). Among the forest sites, YY had the highest annual ET; DX and DHS had intermediate ET; the low-productivity forest site – CBS had the lowest ET. The grassland sites exhibited less cross-site variability in ET, ranging from 200 to 400 mm yr^{-1}. Among the coastal wetlands sites, the mangrove sites (GQ and YX) had higher ET than the salt marsh sites (DT1, DT2, and DT3).

ET exhibited significant interannual variability for some sites (Fig. 5). For example, the maximum annual differences in ET for two forest sites – DX and DHS were 110.7 and 98.0 mm yr^{-1}, which were equivalent to 18.9% and 15.5% of the mean annual ET at these two sites, respectively. Among the grasslands, DL1 exhibited the largest annual difference in ET with a decline of 163.1 mm (or 36.3%) in 2007 relative to 2006. For the cropland site – DL2, annual ET in 2007 was 129 mm (32.9%) lower than that of 2006. Among the salt marsh sites, DT3 had almost identical annual ET for 2005 and 2007; for DT2, ET in 2006 was 82 mm (13.3%) higher than measured in 2005.

Across all the sites, annual ET exhibited a strong decreasing trend with increasing latitude (Fig. 6a). Overall, the tropical and subtropical sites had the highest ET, the temperate sites had the intermediate ET, and the cold temperate, dryland, and subalpine sites had the lowest ET. Annual ET exhibited no clear longitudinal patterns.

3.4. Climate regulation of evapotranspiration (ET) and carbon–water coupling

Annual ET was strongly correlated with annual temperature and precipitation across sites (Fig. 6). Overall, warmer and wetter sites had higher ET, while drier and/or colder sites had lower ET. Compared with precipitation, temperature explained slightly higher variance of ET. There was no significant relationship between annual ET and PAR (or VPD) across sites.

Annual ET was strongly correlated with annual carbon fluxes across sites (Fig. 6). Both GPP and ER were positively related to ET. The strong correlation between GPP and ET demonstrated the coupling of carbon and water cycles for terrestrial ecosystems in China. Annual NEP had a positive relationship with annual ET, indicating that higher net carbon uptake corresponded to higher ET. Overall, higher-productivity sites had higher ET, while lower-productivity sites had lower ET. Annual ET was also positively correlated with GSL across sites (Fig. 6).

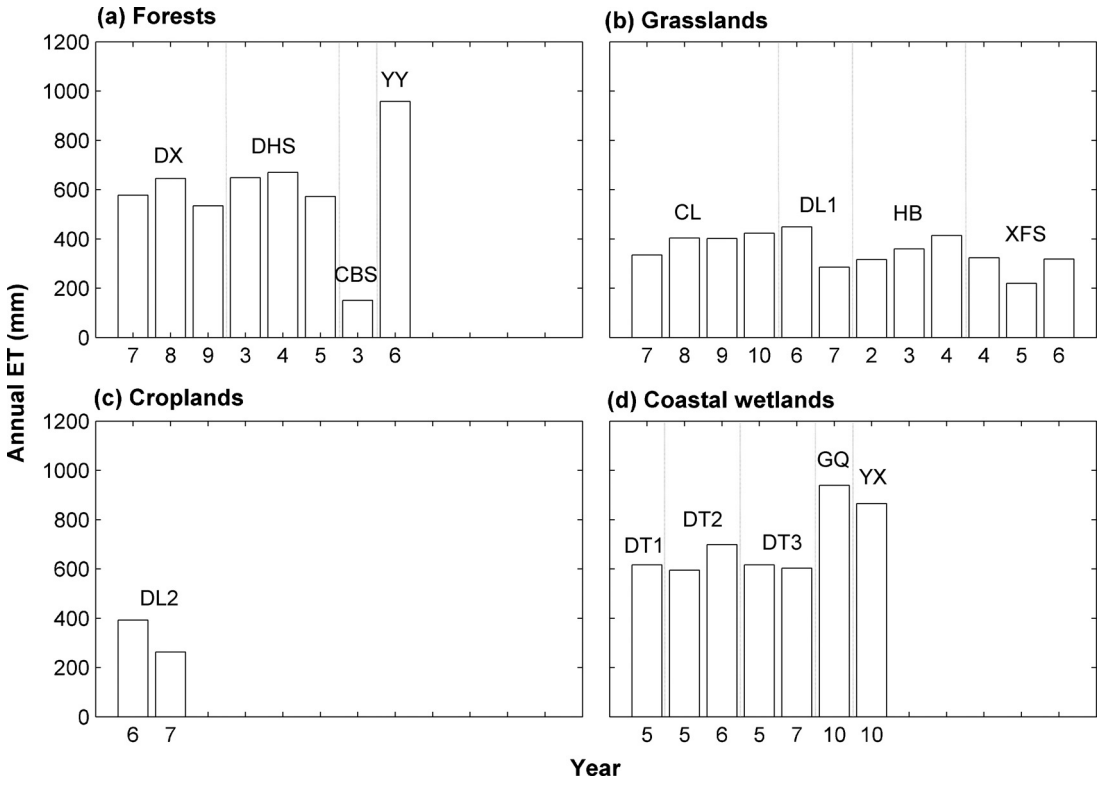

Fig. 5. Annual ET for each eddy covariance site within each vegetation type: (a) forests; (b) grasslands; (c) croplands; (d) coastal wetlands.

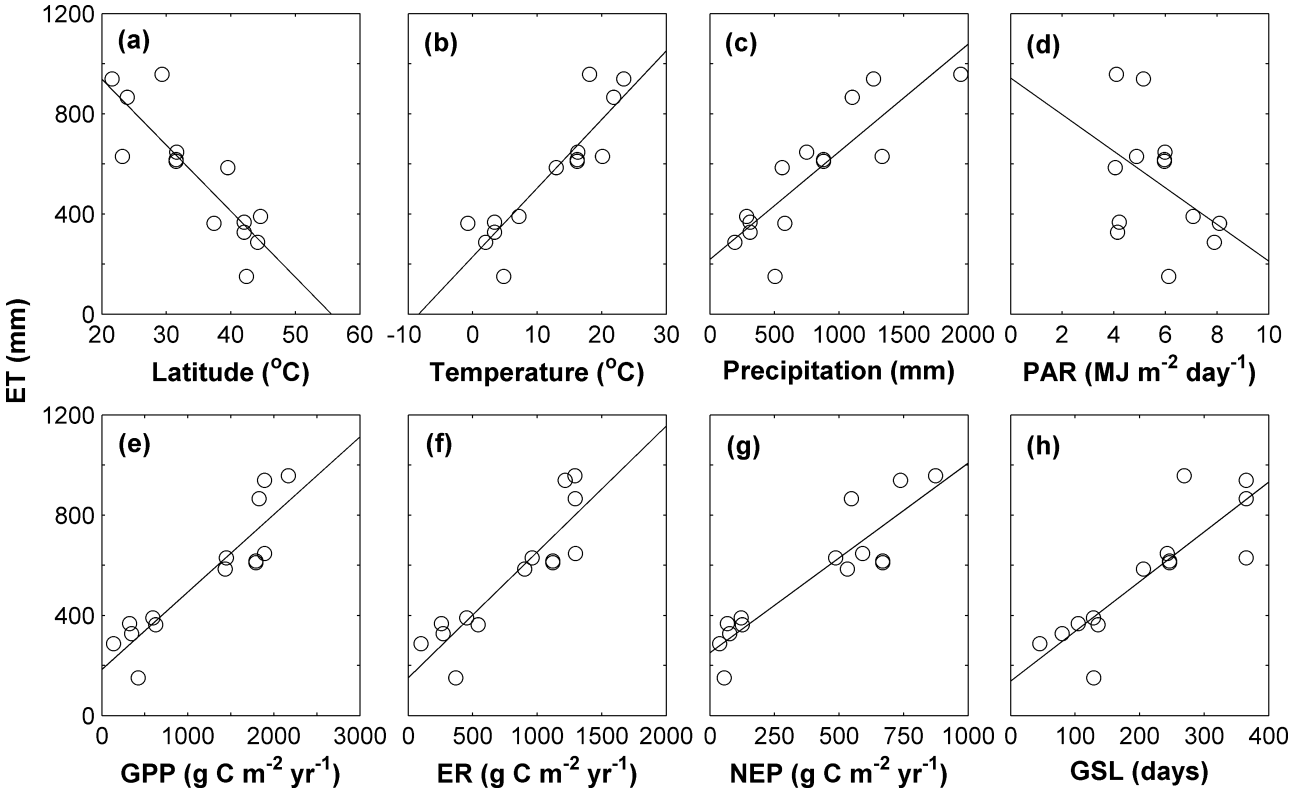

Fig. 6. Relationships of annual ET with latitude, climate variables, and carbon fluxes: top panels – (a) latitude ($y = -26.33x + 1464.42$, $R^2 = 0.74$, $p < 0.001$), (b) annual temperature ($y = 27.38x + 230.29$, $R^2 = 0.80$, $p < 0.001$), (c) annual precipitation ($y = 0.43x + 218.36$, $R^2 = 0.73$, $p < 0.001$), and (d) annual PAR ($y = -73.07x + 942.41$, $R^2 = 0.18$, $p = 0.15$) and bottom panels – (e) annual GPP ($y = 0.31x + 183.77$, $R^2 = 0.83$, $p < 0.001$), (f) annual ER ($y = 0.50x + 150.98$, $R^2 = 0.80$, $p < 0.001$), (g) annual NEP ($y = 0.76x - 250.71$, $R^2 = 0.83$, $p < 0.001$), and (h) GSL ($y = 1.99x + 137.42$, $R^2 = 0.74$, $p < 0.001$).

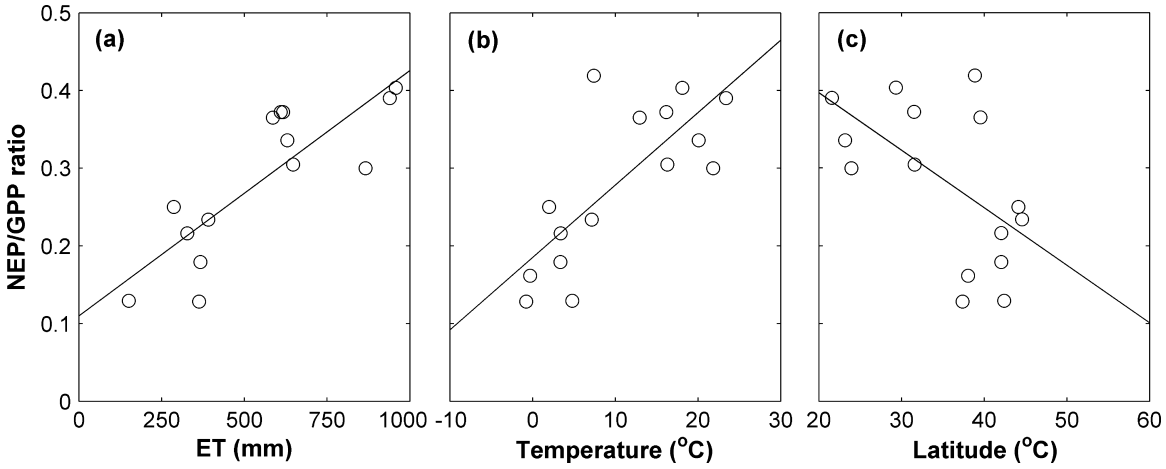

Fig. 7. Relationships of annual NEP/GPP ratio with (a) annual ET ($y = 0.0003x + 0.11$, $R^2 = 0.69$, $p < 0.001$), (b) annual temperature ($y = 0.009x + 0.18$, $R^2 = 0.58$, $p < 0.001$), and (c) latitude ($y = -0.007x + 0.54$, $R^2 = 0.32$, $p < 0.05$) across sites.

Annual ET was positively correlated with the ratio of annual NEP to GPP (NEP/GPP) (Fig. 7a). Ecosystems with higher annual ET had a larger fraction of GPP as net carbon uptake. NEP/GPP was also positively correlated with air temperature (Fig. 7b). NEP/GPP exhibited weak latitudinal dependency (Fig. 7c).

3.5. Water use efficiency (WUE)

Annual WUE varied with site and vegetation type (Fig. 8; Table 3), and ranged from 0.37 to 3.1 g C kg^{-1} H_2O (Fig. 8). The higher-productivity forest and coastal wetland sites generally had higher WUE (~2.0–3.0 g C kg^{-1} H_2O) than the lower-productivity grassland and cropland sites (~0.5–1.0 g C kg^{-1} H_2O) (Fig. 8). Among the forest sites, CBS had slightly higher WUE than other sites. Among the grassland sites, HB had much higher WUE than other sites. For coastal wetlands, the salt marsh ecosystems (DT1, DT2, and DT3) had higher WUE than the mangrove ecosystems (GQ and YX). Five of the 22 sites – GT, KBQ, SZW1, SZW2, and XLH2 had WUE data for the growing season only (Table 3). Over the growing season, GT and XLH2 had relatively high WUE (>3.0 g C kg^{-1} H_2O), while KBQ, SZW1, and SZW2 had relatively low WUE (<1.0 g C kg^{-1} H_2O).

WUE generally exhibited relatively small interannual variability (Fig. 8). For example, WUE was almost identical in all years for CL, HB and DL2. For forest sites, DX had almost identical WUE in 2008 and 2009, while the annual WUE in 2007 was about 11% lower than that of 2008 and 2009. The WUE of DHS in 2005 was 13.3% higher than in 2004. For the salt marsh sites, the WUE of DT2 in 2006 was 12.2% higher than in 2005; the WUE of DT3 in 2007 was also 12.0% higher than in 2005.

Unlike carbon and water fluxes, WUE exhibited no clear latitudinal dependency. There was a strong nonlinear relationship between annual WUE and precipitation across sites (Fig. 9). WUE increased quickly with precipitation when annual precipitation was lower than 500 mm, and tended to saturate when precipitation was above 500 mm. Annual WUE was not significantly correlated with annual temperature across sites. Annual WUE was also nonlinearly related to GSL (Fig. 9).

4. Discussion

4.1. Carbon fluxes

Our results show that annual fluxes varied substantially across ecosystem types in China. Overall, forest and cropland sites had higher annual fluxes than did grassland sites. All sites provided carbon sinks except XLH2. In 2006, XLH2 slightly released carbon into the atmosphere during the growing season likely because of drought stress, and the precipitation during the growing season at this site (~173 mm) was substantially lower than the long-term mean annual precipitation (350 mm).

Our results indicate that the ecosystem carbon sequestration capacity of forest plantations was similar to or slightly higher than that of natural forests. The incorporation of the difference between plantation and natural forests into national-scale estimations will require spatially explicit information on the distribution, location, and age of plantations and natural forests. We only had data from two plantation sites, and therefore could not examine the effect of age on carbon fluxes for plantations. China has the largest area of forest plantations in the world. According to the 7th national forest inventory, China currently has 6.17×10^5 km^2 of forest plantations (State Forestry Administration of China 2010). These plantations likely provide a large fraction of the terrestrial carbon sink in China (Fang et al., 2001; Wang et al., 2007; Piao et al., 2009). Although the carbon sequestration potential of the plantations will eventually decrease as the forests age, forest plantations can provide carbon sinks at decadal scales and slow down the buildup of CO_2 in the atmosphere.

The annual fluxes of coastal wetland sites were similar to or slightly higher than those of forest sites, showing that these coastal wetland ecosystems also had great potential for carbon sequestration. However, it should be noted that tides could laterally transport part of the organic carbon from these coastal wetlands to remote estuaries or open oceans (Chalmers et al., 1985; Valiela et al., 2000). The percentage of the carbon transported by tides and the fate of the transported carbon remain uncertain (Twilley et al., 1992). A part of the transported carbon will be deposited in coastal and shelf sediments and a part of it will likely be emitted as CO_2 to the atmosphere. Overall, the regulation of carbon fluxes in coastal wetland ecosystems by tides is poorly understood and it is challenging to fully assess the carbon sequestration capacity of these ecosystems and the feedbacks to the climate (Guo et al., 2009).

Our results show that annual GPP, ER, and NEP exhibited large spatial gradients from south to north and generally declined with increasing latitude. The latitudinal patterns of carbon fluxes are consistent with previous synthesis studies (Kato and Tang, 2008; Yu et al., 2013). However, unlike the results by Yu et al. (2013), our results did not show longitudinal patterns in carbon fluxes. The latitudinal patterns in annual carbon fluxes in China were mainly controlled by annual temperature, annual precipitation, and GSL.

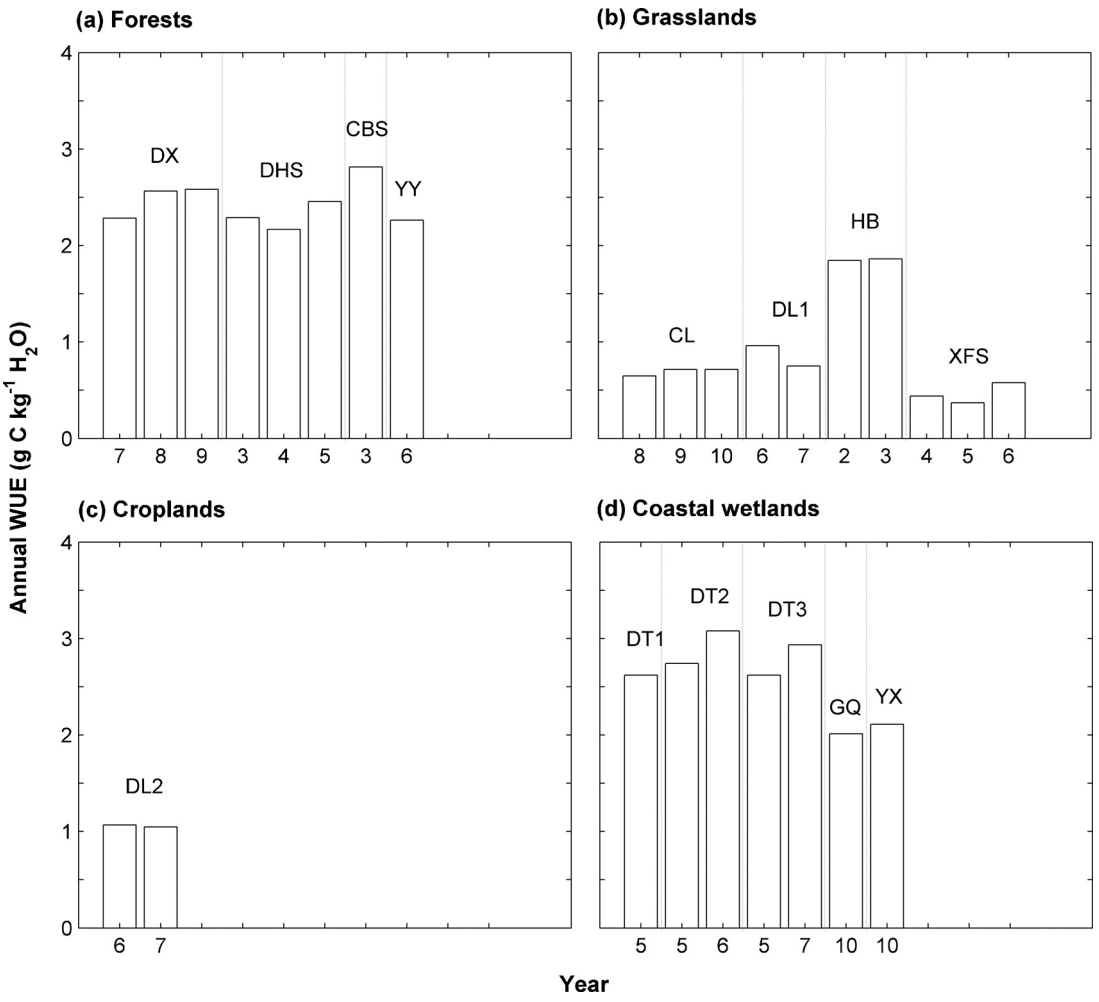

Fig. 8. Annual WUE for each eddy covariance site and each vegetation type: (a) forests; (b) grasslands; (c) croplands; (d) coastal wetlands.

China's terrestrial ecosystems are influenced by the East Asian monsoon. The monsoon leads to a decline in precipitation from the southeast to the northwest, which partly determined the latitudinal dependency of carbon and water fluxes across sites. The decreases in temperature and precipitation with increasing latitude led to the declines in carbon fluxes (Kato and Tang, 2008; Yu et al., 2013). Annual mean temperature had a larger influence on the spatial variation of annual GPP than did annual precipitation. Other climatic factors including PAR and VPD did not play a significant role in controlling the spatial patterns of carbon fluxes. The projected increases in temperature and associated changes in precipitation during the remainder of the 21st century (IPCC, 2007) will likely alter the magnitude and spatial patterns of carbon fluxes of China's terrestrial ecosystems.

The phenological stages (green-up and senescence) and growing season length exhibited latitudinal patterns. The spatial patterns

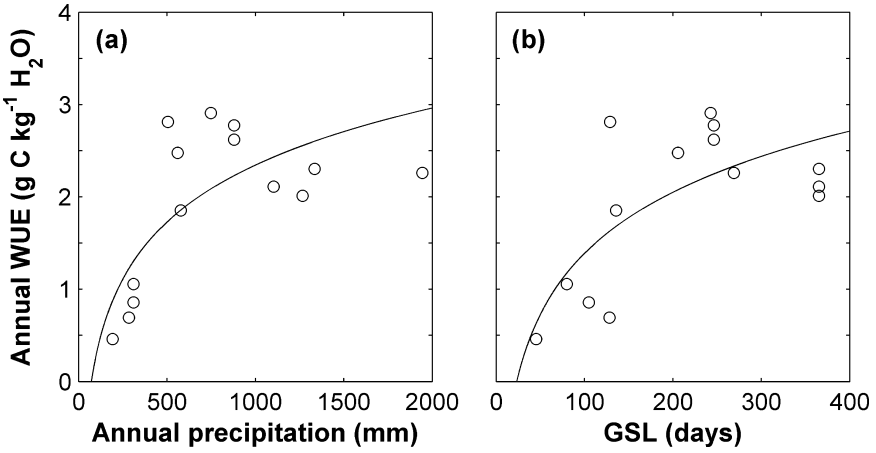

Fig. 9. Relationships of annual WUE with (a) annual precipitation ($y = 0.89 \log(x) - 3.81$, $R^2 = 0.52$, $p < 0.01$) and (b) GSL ($y = 0.95 \log(x) - 3.00$, $R^2 = 0.51$, $p < 0.01$) across sites.

of growing season beginning and end dates were correlated with spatial patterns of mean air temperatures in spring and autumn, respectively (Chen et al., 2005). Our results show that the latitudinal patterns in green-up and senescence dates led to the decline in GSL with increasing latitude. Annual carbon fluxes were strongly correlated with GSL across sites. The lengthening of the GSL resulting from the advancement in green-up date and the delay in senescence date (Chen et al., 2005; Piao et al., 2007; Song et al., 2010) will likely enhance annual GPP and ecosystem carbon sequestration in China.

4.2. Evapotranspiration (ET)

Despite a number of studies on ET for terrestrial ecosystems in China (Gao et al., 2007; Liu et al., 2008; Lei and Yang, 2010; Sun et al., 2011a), the spatial patterns of ET and associated variability across vegetation types have not been well examined (Liu et al., 2012; Lu et al., 2012). Our results show that annual ET generally declined with increasing latitude across sites. The latitudinal dependency of ET was mainly controlled by temperature, precipitation, and GSL. The latitudinal decline in annual temperature and precipitation and the resulting decline in GSL resulted in the latitudinal decline in annual ET, showing that annual ET is generally controlled by energy and water availability (Sun et al., 2011a).

The large variability of annual ET across vegetation types can be attributed to mean annual climate conditions, water supply, and plant functional types, which agrees with previous results (Sun et al., 2011a). The coastal wetland ecosystems had high annual ET because of the high temperatures, abundant water supply from high precipitation and tides, and longer GSL. The semiarid grassland sites generally had low ET mainly because of low precipitation. The subalpine and alpine ecosystems also had relatively low ET because of lower temperatures, shorter GSL, and less precipitation. The interannual variability of ET at a given site was largely driven by the interannual variability of precipitation.

The strong correlation between GPP and ET across sites demonstrated that the carbon and water cycles are tightly coupled. The carbon and water cycles are coupled due to the stomatal control on both carbon and water exchange between ecosystems and the atmosphere through photosynthesis and transpiration (Niu et al., 2008; Chapin et al., 2011). Using simple relationships between monthly GPP and ET, Sun et al. (2011b) provided continental estimate of GPP, ET, and water yield for the U.S. The strong positive relationship of annual ET with the ratio of annual NEP to GPP (NEP/GPP) showed that higher ET corresponded to a higher fraction of net carbon uptake out of GPP. Temperature exhibited a similar relationship with NEP/GPP. The latitudinal patterns of ET and temperature were responsible for the similar latitudinal pattern in NEP/GPP.

4.3. Water use efficiency (WUE)

WUE measures the tradeoff between carbon gain and water loss during photosynthesis and is an important link of the carbon and water cycles (Niu et al., 2008; Chapin et al., 2011). Previous studies examined WUE for individual biomes and for a very limited number of sites in China (Hu et al., 2008; Yu et al., 2008a; Liu et al., 2010). Our study examined the magnitude, spatial patterns, and variability of WUE across 22 sites encompassing a range of ecosystem and climate types.

Our results show substantial variability in annual WUE across vegetation types. Higher WUE corresponded to higher temperature, higher precipitation, and longer GSL. This is consistent with some previous result. Annual WUE ranged between 4.1 and 5.3 g C kg^{-1} H_2O for coastal Douglas-fir stands in the Pacific Northwest (Jassal et al., 2009), and also varied with stand age (Chen et al., 2002; Jassal et al., 2009). Simulations of an ecosystem model showed that the average WUE was about 0.71 g C kg^{-1} H_2O in the southeastern U.S., and WUE varied with biome, ranging from 0.45–0.93 g C kg^{-1} H_2O (Tian et al., 2010). However, some studies showed that WUE was similar between biomes except tundra (e.g., Law et al., 2002).

Several studies examined WUE of terrestrial ecosystems in China. For example, Hu et al. (2008) examined the ecosystem-level WUE within and among four grassland ecosystems in China using the EC technique. Their results suggested that leaf area index (LAI) was the dominant factor controlling the seasonal variations of WUE for these grasslands (Hu et al., 2008). Yu et al. (2008a) examined WUE of three forest ecosystems in eastern China and analyzed its relationships to climatic variables. The mean annual WUE of the three forest ecosystems were between 1.88 and 2.55 g C kg^{-1} H_2O (Yu et al., 2008a). Spring maize on the Less Plateau, China was reported to have slightly different WUE ranging from 2.7 to 3.3 g C kg^{-1} H_2O under different water management practices (Liu et al., 2010). These WUE estimates generally fell within the range based on our synthesis (0.37–3.1 g C kg^{-1} H_2O).

Our results show that the spatial patterns of annual WUE of terrestrial ecosystems were mainly controlled by annual precipitation and growing season length. Previous studies have shown that annual temperature and precipitation were the main factors controlling the spatial pattern of WUE for 3 forest sites in eastern China (Yu et al., 2008a). Experimental results have demonstrated that in the semiarid temperate steppe in China, ecosystem WUE increased by 22.2% under the increased precipitation treatment (Niu et al., 2008). The projected increases in precipitation (IPCC, 2007) will likely increase WUE of China's terrestrial ecosystems, particularly water-limited grassland and cropland ecosystems.

The high GPP and WUE in southern China suggest that efforts to strengthen China's ecosystem carbon sequestration from plantation forests should focus on the southern China where heat and water are ideal for maintaining high productivity. This strategy is especially important because efforts to increase carbon sequestration in areas of limited water may inadvertently contribute to the ongoing water crisis in northern China (Sun et al., 2006).

4.4. Comparison with the globe and other regions in Asia

We compared the annual carbon fluxes, ET, and WUE averaged for all sites in China with averages for the globe and other regions in Asia (Fig. 10). We used mean annual fluxes previously published for the globe (e.g., Yi et al., 2010) and Asia (Kato and Tang, 2008). The average annual GPP and ER of China were slightly lower than those of the globe and Asia. However, the average annual NEP of China was slightly higher than that of the globe and Asia. For forests, China exhibited slightly lower GPP and ER and slightly higher NEP than the globe and Asia. For grasslands, China showed lower carbon fluxes than the globe mainly because the average annual precipitation of the grassland sites in China (360.9 mm) was much lower than that for the globe (877.9 mm). The fluxes were not compared for croplands because we had data from only one cropland site in China. The average annual ET and WUE of China were slightly lower than those of the globe (Fig. 10). For forests, China had similar average annual ET and WUE to the globe; and for grasslands, China had lower average annual ET and WUE than the globe. Overall, the differences in carbon fluxes, ET, and WUE between China and the globe (or other regions in Asia) were generally not statistically significant.

We examined the latitudinal patterns and climatic controls of annual carbon fluxes, ET, and WUE for sites across the globe. Unlike China, the globe exhibited no latitudinal patterns in annual carbon fluxes and WUE. Similar to China, the globe exhibited correlations between annual ET and latitude ($y = -15.40x + 1210.72$, $R^2 = 0.42$, $p < 0.001$). For all global sites, annual GPP had relatively weak to moderate correlations with temperature ($y = 49.02x + 696.02$,

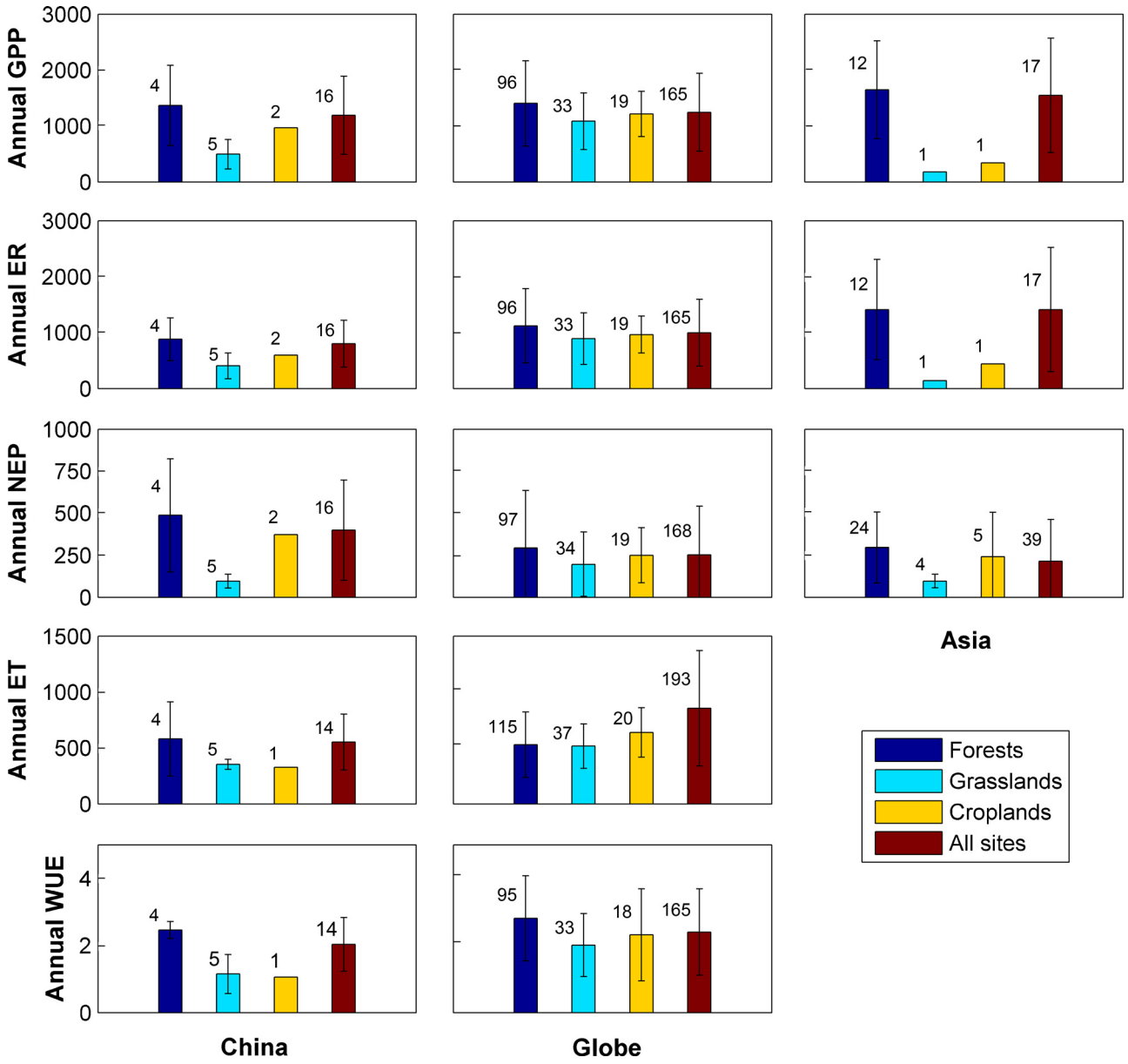

Fig. 10. Annual carbon fluxes (g C m^{-2} yr^{-1}), ET (mm yr^{-1}), and WUE (g C kg^{-1} H_2O) averaged for all sites in China, the globe, and Asia. The data were obtained from Yi et al. (2010) for sites over the globe and Kato and Tang (2008) for sites in Asia. The sites of China are excluded for the calculation of the average carbon fluxes, ET, and WUE for the globe and Asia. The error bars stand for the standard deviation among sites. The numbers by the bars stand for the number of sites used for the calculation of the means and standard deviation. Standard deviation was not calculated if the number of sites was fewer than 3.

$R^2 = 0.25$, $p < 0.001$) and precipitation ($y = 0.78x + 518.05$, $R^2 = 0.39$, $p < 0.001$); annual ER was also significantly, but weakly, correlated with temperature ($y = 35.48x + 595.04$, $R^2 = 0.17$, $p < 0.001$) and precipitation ($y = 0.61x + 426.75$, $R^2 = 0.31$, $p < 0.001$); annual NEP had very weak correlations with both temperature and precipitation ($R^2 < 0.1$). Annual ET had moderate to weak correlations with temperature ($y = 24.15x + 283.91$, $R^2 = 0.39$, $p < 0.001$) and precipitation ($y = 0.26x + 291.51$, $R^2 = 0.29$, $p < 0.001$). The global relationships between the carbon/water fluxes and climate factors were generally much weaker than those for China. The majority of the sites for China are located in the eastern half of the country where the climate is strongly influenced by the East Asian monsoon, and both temperature and precipitation exhibited strong latitudinal dependency. Globally, precipitation exhibits no clear spatial pattern although temperature generally declines with latitude. For example, eastern North America and Europe have much higher annual precipitation than similar latitudes in western North America and central Asia. The differences in the spatial patterns of climate factors mainly resulted in the differences in the relationships of carbon/water fluxes with climate factors between the China and the Globe.

We also analyzed the latitudinal patterns and climatic controls of carbon fluxes for other regions in Asia. Similar to China, Asia exhibited strong latitudinal dependency for both annual GPP ($y = -48.93x + 3080.54$, $R^2 = 0.77$, $p < 0.001$) and ER ($y = -52.05x + 3036.29$, $R^2 = 0.74$, $p < 0.001$); unlike China, Asia showed no latitudinal dependency for annual NEP. GPP was strongly correlated with temperature ($y = 88.69x + 437.76$, $R^2 = 0.74$, $p < 0.001$) and precipitation ($y = 0.90x + 303.01$, $R^2 = 0.51$, $p < 0.001$); ER was also strongly or moderately related to temperature ($y = 92.04x + 252.26$, $R^2 = 0.69$, $p < 0.001$) and precipitation ($y = 0.89x + 167.84$, $R^2 = 0.44$, $p < 0.001$). These correlations for Asia

were generally as strong as those for China. However, unlike China, Asia exhibited no correlations between annual NEP and temperature/precipitation.

It should be noted that although we made use of observations from 22 sites, the number of sites is still limited, particularly for croplands. Globally, we used data from 193 sites for comparison, but many geographical regions and some vegetation/climate types are still underrepresented. Therefore, the differences in carbon fluxes, ET, and WUE observed between China and the globe (or other regions in Asia) (Fig. 10) and the relationships of these variables with latitude and climate factors described above should be interpreted with caution, and these differences and relationships will likely be altered by the availability of flux observations from more sites in the future.

5. Conclusions

We synthesized flux and micrometeorological observations from 22 EC flux sites encompassing a range of climate and ecosystem types across China, and examined the magnitude, spatial patterns, and climate regulation of carbon fluxes (GPP, ER, and NEP), ET, and WUE. Our results show that annual carbon and water fluxes declined with increasing latitude. The latitudinal patterns of carbon and water fluxes were mainly regulated by annual temperature, precipitation, and growing season length. Annual WUE of terrestrial ecosystems were mainly controlled by annual precipitation and growing season length. Carbon fluxes, ET, and WUE varied with ecosystem type. Overall, forest and coastal wetland sites had higher carbon and water fluxes as well as WUE than grassland and cropland sites. Forest plantations had high carbon sequestration capacity, and plantations across the country likely provide a significant carbon sink. Efforts to strengthen China's ecosystem carbon sequestration should focus on ecosystems such as forest plantations in southern China where heat and water are ideal for maintaining high productivity, and this strategy is especially important because efforts to increase carbon sequestration in areas of limited water may inadvertently contribute to the ongoing water crisis in northern China. The coastal salt marsh and mangroves sites were also highly productive and had high carbon sequestration capacity. The strong correlations between annual carbon fluxes and ET across sites show that the carbon and water cycles are tightly coupled. Carbon and water balances in China are highly controlled by precipitation and air temperature. Therefore, future changes in climate will likely alter carbon sequestration capacity and ET of terrestrial ecosystems in China.

Author contributions

JX designed the study, conducted the research, and wrote the paper; JX, GS, and JC promoted the sharing of data across USCCC; GS, JC, HG, SM, and GZ provided comments that improved the manuscript; HC, SC, GD, SG, HG, JG, SH, TK, YL, GL, WL, MM, CS, XW, XX, XZ, ZZ, BZ, GZ, and JZ contributed data; authors from HC to JZ are listed alphabetically.

Acknowledgements

This work is partly supported by the National Science Foundation through the MacroSystems Biology Program (award number 1065777, JX), the National Aeronautics and Space Administration (NASA) through the Carbon Monitoring System (CMS) program (award number NNX11AL32G, JX), and the Department of Energy (DOE) through the National Institute for Climatic Change Research (NICCR) (award number 14U776, JX). This is the first cross-site synthesis paper of the U.S.–China Carbon Consortium (USCCC). We thank the two anonymous reviewers for their constructive and detailed comments on earlier versions of the manuscript.

References

Amiro, B.D., Barr, A.G., Barr, J.G., Black, T.A., Bracho, R., Brown, M., Chen, J., Clark, K.L., Davis, K.J., Desai, A.R., Dore, S., Engel, V., Fuentes, J.D., Goldstein, A.H., Goulden, M.L., Kolb, T.E., Lavigne, M.B., Law, B.E., Margolis, H.A., Martin, T., McCaughey, J.H., Misson, L., Montes-Helu, M., Noormets, A., Randerson, J.T., Starr, G., Xiao, J., 2010, G00K02. Ecosystem carbon dioxide fluxes after disturbance in forests of North America. J. Geophys. Res. 115, http://dx.doi.org/10.1029/2010JG001390.

Baldocchi, D., 2008. Breathing of the terrestrial biosphere: lessons learned from a global network of carbon dioxide flux measurement systems. Aust. J. Bot. 56, 1–26.

Baldocchi, D., Falge, E., Gu, L.H., Olson, R., Hollinger, D., Running, S., Anthoni, P., Bernhofer, C., Davis, K., Evans, R., Fuentes, J., Goldstein, A., Katul, G., Law, B., Lee, X.H., Malhi, Y., Meyers, T., Munger, W., Oechel, W.U., Pilegaard, K.T.P., Schmid, K., Valentini, H.P., Verma, R., Vesala, S., Wilson, T., Wofsy, K.S., 2001. FLUXNET: a new tool to study the temporal and spatial variability of ecosystem-scale carbon dioxide, water vapor, and energy flux densities. Bull. Am. Meteorol. Soc. 82, 2415–2434.

Beer, C., Ciais, P., Reichstein, M., Baldocchi, D., Law, B.E., Papale, D., Soussana, J.F., Ammann, C., Buchmann, N., Frank, D., Gianelle, D., Janssens, I.A., Knohl, A., Kostner, B., Moors, E., Roupsard, O., Verbeeck, H., Vesala, T., Williams, C.A., Wohlfahrt, G., 2009, GB2018. Temporal and among-site variability of inherent water use efficiency at the ecosystem level. Global Biogeochem. Cycles 23, http://dx.doi.org/10.1029/2008GB003233.

Chalmers, A.G., Wiegert, R.G., Wolf, P.L., 1985. Carbon balance in a salt-marsh – interactions of diffusive export tidal deposition and rainfall-caused erosion. Estuar. Coast. Shelf Sci. 21, 757–771.

Chapin, F.S., Matson, P.A., Vitousek, P.M., 2011. Principles of Terrestrial Ecosystem Ecology, 2nd ed. Springer, New York.

Chen, J.Q., Falk, M., Euskirchen, E.U.K.T.P., Suchanek, T.H., Ustin, S.L., Bond, B.J., Brosofske, K.D., Phillips, N., Bi, R.C., 2002. Biophysical controls of carbon flows in three successional Douglas-fir stands based on eddy-covariance measurements. Tree Physiol. 22, 169–177.

Chen, S.P., Chen, J.Q., Lin, G.H., Zhang, W.L., Miao, H.X., Wei, L., Huang, J.H., Han, X.G., 2009. Energy balance and partition in Inner Mongolia steppe ecosystems with different land use types. Agric. For. Meteorol. 149, 1800–1809.

Chen, X.Q., Hu, B., Yu, R., 2005. Spatial and temporal variation of phenological growing season and climate change impacts in temperate eastern China. Glob. Change Biol. 11, 1118–1130.

Dong, G., Guo, J.X., Chen, J.Q., Sun, G., Gao, S., Hu, L.J., Wang, Y.L., 2011. Effects of spring drought on carbon sequestration, evapotranspiration and water use efficiency in the Songnen Meadow Steppe in Northeast China. Ecohydrology 4, 211–224.

Fang, J.Y., Chen, A.P., Peng, C.H., Zhao, S.Q., Ci, L., 2001. Changes in forest biomass carbon storage in China between 1949 and 1998. Science 292, 2320–2322.

Friedl, M.A., McIver, D.K., Hodges, J.C.F., Zhang, X.Y., Muchoney, D., Strahler, A.H., Woodcock, C.E., Gopal, S., Schneider, A., Cooper, A., Baccini, A., Gao, F., Schaaf, C., 2002. Global land cover mapping from MODIS: algorithms and early results. Rem. Sens. Environ. 83, 287–302.

Gao, G., Chen, D.L., Xu, C.Y., Simelton, E., 2007, D11120. Trend of estimated actual evapotranspiration over China during 1960–2002. J. Geophys. Res. 112, http://dx.doi.org/10.1029/2006JD008010.

Guan, D.X., Wu, J.B., Zhao, X.S., Han, S.J., Yu, G.R., Sun, X.M., Jin, C.J., 2006. CO_2 fluxes over an old temperate mixed forest in northeastern China. Agric. For. Meteorol. 137, 138–149.

Guo, H.Q., Noormets, A., Zhao, B., Chen, J.Q., Sun, G., Gu, Y.J., Li, B., Chen, J.K., 2009. Tidal effects on net ecosystem exchange of carbon in an estuarine wetland. Agric. For. Meteorol. 149, 1820–1828.

Hu, Z.M., Yu, G.R., Fu, Y.L., Sun, X.M., Li, Y.N., Shi, P.L., Wangw, Y.F., Zheng, Z.M., 2008. Effects of vegetation control on ecosystem water use efficiency within and among four grassland ecosystems in China. Glob. Change Biol. 14, 1609–1619.

IPCC, 2007. Climate Change 2007 – The Physical Science Basis, 2007. Contribution of Working Group I to the Fourth Assessment Report of the IPCC. Cambridge University Press, New York.

Jassal, R.S., Black, T.A., Spittlehouse, D.L., Brummer, C., Nesic, Z., 2009. Evapotranspiration and water use efficiency in different-aged Pacific Northwest Douglas-fir stands. Agric. For. Meteorol. 149, 1168–1178.

Kato, T., Tang, Y.H., 2008. Spatial variability and major controlling factors of CO_2 sink strength in Asian terrestrial ecosystems: evidence from eddy covariance data. Glob. Change Biol. 14, 2333–2348.

Kato, T., Tang, Y.H., Gu, S., Cui, X.Y., Hirota, M., Du, M.Y., Li, Y.N., Zhao, Z.Q., Oikawa, T., 2004. Carbon dioxide exchange between the atmosphere and an alpine meadow ecosystem on the Qinghai-Tibetan Plateau, China. Agric. For. Meteorol. 124, 121–134.

Kato, T., Tang, Y.H., Gu, S., Hirota, M., Du, M.Y., Li, Y.N., Zhao, X.Q., 2006. Temperature and biomass influences on interannual changes in CO_2 exchange in an alpine meadow on the Qinghai-Tibetan Plateau. Glob. Change Biol. 12, 1285–1298.

Khatun, R.O.T., Kotani, A., Asanuma, J., Gamo, M., Han, S., Hirano, T., Nakai, Y., Saigusa, N., Takagi, K., Wang, H., Yoshifuji, N., 2011. Spatial variations in evapotranspiration over East Asian forest sites. I. Evapotranspiration and decoupling coefficient. Hydrol. Res. Lett. 5, 83–87.

Law, B.E., Falge, E., Gu, L., Baldocchi, D.D., Bakwin, P., Berbigier, P., Davis, K., Dolman, A.J., Falk, M., Fuentes, J.D., Goldstein, A., Granier, A., Grelle, A., Hollinger,

D., Janssens, I.A., Jarvis, P., Jensen, N.O., Katul, G., Mahli, Y., Matteucci, G., Meyers, T., Monson, R., Munger, W., Oechel, W., Olson, R., Pilegaard, K., Paw U, K.T., Thorgeirsson, H., Valentini, R., Verma, S., Vesala, T., Wilson, K., Wofsy, S., 2002. Environmental controls over carbon dioxide and water vapor exchange of terrestrial vegetation. Agric. For. Meteorol. 113, 97–120.

Lei, H.M., Yang, D.W., 2010. Interannual and seasonal variability in evapotranspiration and energy partitioning over an irrigated cropland in the North China Plain. Agric. For. Meteorol. 150, 581–589.

Li, Y.L., Zhou, G.Y., Zhang, D.Q., Wenigmann, K.O., Otieno, D., Tenhunen, J., Zhang, Q.M., Yan, J.H., 2012. Quantification of ecosystem carbon exchange characteristics in a dominant subtropical evergreen forest ecosystem. Asia-Pac. J. Atmos. Sci. 48, 1–10.

Liu, C., Zhang, Z., Sun, G., Zha, T., Zhu, J., Shen, L., Chen, J., Fang, X., Chen, J., 2009. Quantifying evapotranspiration and biophysical regulations of a poplar plantation assessed by eddy covariance and sap-flow methods. Chin. J. Plant Ecol. 33, 706–718.

Liu, M.L., Tian, H.Q., Chen, G.S., Ren, W., Zhang, C., Liu, J.Y., 2008. Effects of land-use and land-cover change on evapotranspiration and water yield in China during 1900–2000. J. Am. Water Resour. Assoc. 44, 1193–1207.

Liu, M.L., Tian, H.Q., Lu, C.Q., Xu, X.F., Chen, G.S., Ren, W., 2012. Effects of multiple environment stresses on evapotranspiration and runoff over eastern China. J. Hydrol. 426, 39–54.

Liu, Y., Li, S.Q., Chen, F., Yang, S.J., Chen, X.P., 2010. Soil water dynamics and water use efficiency in spring maize (*Zea mays* L.) fields subjected to different water management practices on the Loess Plateau, China. Agric. Water Manage. 97, 769–775.

Lu, Y.H., Fu, B.J., Feng, X.M., Zeng, Y., Liu, Y., Chang, R.Y., Sun, G., Wu, B.F., 2012. A policy-driven large scale ecological restoration: quantifying ecosystem services changes in the Loess Plateau of China. PLoS ONE 7, e31782.

Niu, S.L., Wu, M.Y., Han, Y., Xia, J.Y., Li, L.H., Wan, S.Q., 2008. Water-mediated responses of ecosystem carbon fluxes to climatic change in a temperate steppe. New Phytol. 177, 209–219.

Pan, Y.D., Birdsey, R.A., Fang, J.Y., Houghton, R., Kauppi, P.E., Kurz, W.A., Phillips, O.L., Shvidenko, A., Lewis, S.L., Canadell, J.G., Ciais, P., Jackson, R.B., Pacala, S.W., McGuire, A.D., Piao, S.L., Rautiainen, A., Sitch, S., Hayes, D., 2011. A large and persistent carbon sink in the world's forests. Science 333, 988–993.

Paw U, K.T., 2006. Unifying biomicrometeorological measurements. Agric. For. Meteorol. 137, 121–122.

Piao, S.L., Fang, J.Y., Ciais, P., Peylin, P., Huang, Y., Sitch, S., Wang, T., 2009. The carbon balance of terrestrial ecosystems in China. Nature 458, 1009–1082.

Piao, S.L., Friedlingstein, P., Ciais, P., Viovy, N., Demarty, J., 2007, GB3018. Growing season extension and its impact on terrestrial carbon cycle in the Northern Hemisphere over the past 2 decades. Global Biogeochem. Cycles 21, http://dx.doi.org/10.1029/2006GB002888.

Ponton, S., Flanagan, L.B., Alstad, K.P., Johnson, B.G., Morgenstern, K., Kljun, N., Black, T.A., Barr, A.G., 2006. Comparison of ecosystem water-use efficiency among Douglas-fir forest aspen forest and grassland using eddy covariance and carbon isotope techniques. Glob. Change Biol. 12, 294–310.

Ryu, Y., Baldocchi, D.D., Ma, S., Hehn, T., 2008, D09104. Interannual variability of evapotranspiration and energy exchange over an annual grassland in California. J. Geophys. Res. 113, http://dx.doi.org/10.1029/2007JD009263.

Schwalm, C.R., Williams, C.A., Schaefer, K., Arneth, A., Bonal, D., Buchmann, N., Chen, J.Q., Law, B.E., Lindroth, A., Luyssaert, S., Reichstein, M., Richardson, A.D., 2010. Assimilation exceeds respiration sensitivity to drought: a FLUXNET synthesis. Glob. Change Biol. 16, 657–670.

Shao, C., Chen, J., Li, L., 2013. Grazing alters the biophysical regulation of carbon fluxes in a desert steppe. Environ. Res. Lett. 8, 025012, 10.1088/1748-9326/8/2/025012.

Song, Y.L., Linderholm, H.W., Chen, D.L., Walther, A., 2010. Trends of the thermal growing season in China 1951–2007. Int. J. Climatol. 30, 33–43.

Sun, G., Alstad, K., Chen, J.Q., Chen, S.P., Ford, C.R., Lin, G.H., Liu, C.F., Lu, N., McNulty, S.G., Miao, H.X., Noormets, A., Vose, J.M., Wilske, B., Zeppel, M., Zhang, Y., Zhang, Z.Q., 2011a. A general predictive model for estimating monthly ecosystem evapotranspiration. Ecohydrology 4, 245–255.

Sun, G., Caldwell, P., Noormets, A., McNulty, S.G., Cohen, E., Myers, J.M., Domec, J.C., Treasure, E., Mu, Q.Z., Xiao, J.F., John, R., Chen, J.Q., 2011, G00J05. Upscaling key ecosystem functions across the conterminous United States by a water-centric ecosystem model. J. Geophys. Res., http://dx.doi.org/10.1029/2010JG001573.

Sun, G., Sun, J.X., Zhou, G.S., 2009. Water and carbon dynamics in selected ecosystems in China. Agric. For. Meteorol. 149, 1789–1790.

Sun, G., Zhou, G.Y., Zhang, Z.Q., Wei, X.H., McNulty, S.G., Vose, J.M., 2006. Potential water yield reduction due to forestation across China. J. Hydrol. 328, 548–558.

Tian, H.Q., Chen, G.S., Liu, M.L., Zhang, C., Sun, G., Lu, C.Q., Xu, X.F., Ren, W., Pan, S.F., Chappelka, A., 2010. Model estimates of net primary productivity evapotranspiration, and water use efficiency in the terrestrial ecosystems of the southern United States during 1895–2007. For. Ecol. Manage. 259, 1311–1327.

Tian, H.Q., Melillo, J., Lu, C.Q., Kicklighter, D., Liu, M.L., Ren, W., Xu, X.F., Chen, G.S., Zhang, C., Pan, S.F., Liu, J.Y., Running, S., 2011. China's terrestrial carbon balance: contributions from multiple global change factors. Global Biogeochem. Cycles 25, http://dx.doi.org/10.1029/2010GB003838, GB1007.

Twilley, R.R., Chen, R.H., Hargis, T., 1992. Carbon sinks in mangroves and their implications to carbon budget of tropical coastal ecosystems. Water Air Soil Pollut. 64, 265–288.

Valiela, I., Cole, M.L., McClelland, J., Hauxwell, J., Cebrian, J., Joye, S.B., 2000. Role of salt marshes as part of coastal landscape. In: Weinstein, M.P., Kreeger, D.A. (Eds.), Concepts and Controversies in Tidal Marsh Ecology. Kluwer Academic Publishers, Dordrecht, pp. 23–38.

Wang, S., Chen, J.M., Ju, W.M., Feng, X., Chen, M., Chen, P., Yu, G., 2007. Carbon sinks and sources in China's forests during 1901–2001. J. Environ. Manage. 85, 524–537.

Wang, X.F., Ma, M.G., Huang, G.H., Veroustraete, F., Zhang, Z.H., Song, Y., Tan, J.L., 2012. Vegetation primary production estimation at maize and alpine meadow over the Heihe River Basin, China. Int. J. Appl. Earth Obs. Geoinf. 17, 94–101.

Wang, Y.L., Zhou, G.S., Wang, Y.H., 2008. Environmental effects on net ecosystem CO(2) exchange at half-hour and month scales over Stipa krylovii steppe in northern China. Agric. For. Meteorol. 148, 714–722.

Wei, X., Liu, S., Zhou, G., Wang, C., 2005. Hydrological processes in major types of Chinese forest. Hydrol. Process. 19, 63–75.

Wei, Y., Gao, S., Zhang, X., Geng, S., Zhao, X., Jiang, Z., Wang, Y., 2012. Source area in-FLUX measurements by FSAM model over the *Populus deltoides* plantation in Yueyang. Sci. Silv. Sin. 48, 16–21.

Wilske, B., Lu, N., Wei, L., Chen, S.P., Zha, T.G., Liu, C.F., Xu, W.T., Noormets, A., Huang, J.H., Wei, Y.F., Chen, J., Zhang, Z.Q., Ni, J., Sun, G., Guo, K., McNulty, S., John, R., Han, X.G., Lin, G.H., Chen, J.Q., 2009. Poplar plantation has the potential to alter the water balance in semiarid Inner Mongolia. J. Environ. Manage. 90, 2762–2770.

Wofsy, S.C., Goulden, M.L., Munger, J.W., Fan, S.M., Bakwin, P.S., Daube, B.C., Bassow, S.L., Bazzaz, F.A., 1993. Net exchange of CO_2 in a midlatitude forest. Science 260, 1314–1317.

Xiao, J.F., Zhuang, Q.L., Baldocchi, D.D., Law, B.E., Richardson, A.D., Chen, J.Q., Oren, R., Starr, G., Noormets, A., Ma, S.Y., Verma, S.B., Wharton, S., Wofsy, S.C., Bolstad, P.V., Burns, S.P., Cook, D.R., Curtis, P.S., Drake, B.G., Falk, M., Fischer, M.L., Foster, D.R., Gu, L.H., Hadley, J.L., Hollinger, D.Y., Katul, G.G., Litvak, M., Martin, T.A., Matamala, R., McNulty, S., Meyers, T.P., Monson, R.K., Munger, J.W., Oechel, W.C. U.K.T.P., Schmid, H.P., Scott, R.L., Sun, G., Suyker, A.E., Torn, M.S., 2008. Estimation of net ecosystem carbon exchange for the conterminous United States by combining MODIS and AmeriFlux data. Agric. For. Meteorol. 148, 1827–1847.

Xiao, J., Zhuang, Q., Law, B.E., Chen, J., Baldocchi, D.D., Cook, D.R., Oren, R., Richardson, A.D., Wharton, S., Ma, S., Martin, T.A., Verma, S.B., Suyker, A.E., Scott, R.L., Monson, R.K., Litvak, M., Hollinger, D.Y., Sun, G., Davis, K.J., Bolstad, P.V., Burns, S.P., Curtis, P.S., Drake, B.G., Falk, M., Fischer, M.L., Foster, D.R., Gu, L., Hadley, J.L., Katul, G.G., Matamala, R., McNulty, S., Meyers, T.P., Munger, J.W., Noormets, A., Oechel, W.C., Paw U, K.T., Schmid, H.P., Starr, G., Torn, M.S., Wofsy, S.C., 2010. A continuous measure of gross primary production for the conterminous U S. derived from MODIS and AmeriFlux data. Rem. Sens. Environ. 114, 576–591.

Xiao, J.F., Zhuang, Q.L., Law, B.E., Baldocchi, D.D., Chen, J.Q., Richardson, A.D., Melillo, J.M., Davis, K.J., Hollinger, D.Y., Wharton, S., Oren, R., Noormets, A., Fischer, M.L., Verma, S.B., Cook, D.R., Sun, G., McNulty, S., Wofsy, S.C., Bolstad, P.V., Burns, S.P., Curtis, P.S., Drake, B.G., Falk, M., Foster, D.R., Gu, L.H., Hadley, J.L., Katulk, G.G., Litvak, M., Ma, S.Y., Martinz, T.A., Matamala, R., Meyers, T.P., Monson, R.K., Munger, J.W., Oechel, W.C., Paw U, K.T., Schmid, H.P., Scott, R.L., Starr, G., Suyker, A.E., Torn, M.S., 2011. Assessing net ecosystem carbon exchange of U.S. terrestrial ecosystems by integrating eddy covariance flux measurements and satellite observations. Agric. For. Meteorol. 151, 60–69.

Xiao, J., Chen, J., Davis, K.J., Reichstein, M., 2012. Advances in upscaling of eddy covariance measurements of carbon and water fluxes. J. Geophys. Res. 117, http://dx.doi.org/10.1029/2011JG001889, G00J01.

Xiao, J.F., Zhuang, Q.L., Liang, E.Y., McGuire, A.D., Moody, A., Kicklighter, D.W., Shao, X.M., Melillo, J.M., 2009. Twentieth-century droughts and their impacts on terrestrial carbon cycling in China. Earth Interact. 13, 1–31, http://dx.doi.org/10.1175/2009EI275.1.

Yan, Y., Zhao, B., Chen, J.Q., Guo, H.Q., Gu, Y.J., Wu, Q.H., Li, B., 2008. Closing the carbon budget of estuarine wetlands with tower-based measurements and MODIS time series. Glob. Change Biol. 14, 1690–1702.

Yi, C.X., et al., 2010. Climate control of terrestrial carbon exchange across biomes and continents. Environ. Res. Lett. 5, 10.1088/1748-9326/5/3/034007.

Yu, G.R., Song, X., Wang, Q.F., Liu, Y.F., Guan, D.X., Yan, J.H., Sun, X.M., Zhang, L.M., Wen, X.F., 2008a. Water-use efficiency of forest ecosystems in eastern China and its relations to climatic variables. New Phytol. 177, 927–937.

Yu, G.R., Wen, X.F., Sun, X.M., Tanner, B.D., Lee, X.H., Chen, J.Y., 2006. Overview of ChinaFLUX and evaluation of its eddy covariance measurement. Agric. For. Meteorol. 137, 125–137.

Yu, G.R., Zhang, L.M., Sun, X.M., Fu, Y.L., Wen, X.F., Wang, Q.F., Li, S.G., Ren, C.Y., Song, X., Liu, Y.F., Han, S.J., Yan, J.H., 2008b. Environmental controls over carbon exchange of three forest ecosystems in eastern China. Glob. Change Biol. 14, 2555–2571.

Yu, G.R., Zhu, X.J., Fu, Y.L., He, H.L., Wang, Q.F., Wen, X.F., Li, X.R., Zhang, L.M., Zhang, L., Su, W., Li, S.G., Sun, X.M., Zhang, Y.P., Zhang, J.H., Yan, J.H., Wang, H.M., Zhou, G.S., Jia, B.R., Xiang, W.H., Li, Y.N., Zhao, L., Wang, Y.F., Shi, P.L., Chen, S.P., Xin, X.P., Zhao, F.H., Wang, Y.Y., Tong, C.L., 2013. Spatial patterns and climate drivers of carbon fluxes in terrestrial ecosystems of China. Glob. Change Biol. 19, 798–810.

Zhou, G.Y., Wei, X.H., Wu, Y.P., Liu, S.G., Huang, Y.H., Yan, J.H., Zhang, D.Q., Zhang, Q.M., Liu, J.X., Meng, Z., Wang, C.L., Chu, G.W., Liu, S.Z., Tang, X.L., Liu, X.D., 2011. Quantifying the hydrological responses to climate change in an intact forested small watershed in Southern China. Glob. Change Biol. 17, 3736–3746.